Determining the role of the *Xist* non-coding RNA in Epigenetic Programming of X-chromosome Inactivation

Lucy Haizlip Williams

A dissertation submitted to the faculty of the University of North Carolina at Chapel Hill in partial fulfillment of the requirements for the degree of Doctor of Philosophy in the Curriculum of Genetics and Molecular Biology.

Chapel Hill
2011

Approved By:

Dr. Terry Magnuson

Dr. Larysa Pevny

Dr. Fernando Pardo-Manuel de Villena

Dr. Scott Bultman

Dr. A. Gregory Matera

Dr. Brian Strahl

Abstract

Lucy Haizlip Williams: Determining the Role of the *Xist* non-coding RNA in Epigenetic Programming of X-chromosome Inactivation
(Under the direction of Terry Magnuson)

Repression of *Xist* RNA expression is considered a prerequisite to reversing X-chromosome inactivation (XCI) in the mouse inner cell mass (ICM), and reactivation of X-linked genes is thought to follow loss of *Xist* RNA coating and heterochromatic markers of inactivation, such as methylation of histone H3. I analyzed X-chromosome activity in developing ICMs and show reactivation of gene expression from the inactive-X initiates in the presence of *Xist* coating and H3K27me3. Furthermore, depletion of *Xist* RNA coating through forced upregulation of NANOG does not result in altered reactivation kinetics. Taken together, our observations suggest that in the ICM, X-linked gene transcription and *Xist* coating are uncoupled. These data fundamentally alter our perception of the reactivation process and support the existence of a mechanism to reactivate Xp-linked genes that operates independent of loss of *Xist* RNA and H3K27me3 from the inactive-X.

Acknowledgements

I would like to acknowledge Dr. Terry Magnuson for his support and guidance through the entirety of my thesis research. Without his confidence in my abilities and daily encouragement, the work presented herein would not have been possible. I would like to thank Dr. Larysa Pevny and Dr. Kat Hadjantonakis whose productive collaborations were essential for many aspects of my thesis research. I am also grateful to Dr. Sundeep Kalantry, whose rigorous interactions pushed me to be a better scientist, and Dr. Stormy Chamberlain who taught me, as a young scientist, to trust my research instincts. To all members of the Magnuson lab, thank you for your friendships; you all made lab a fun place to work!

Table of Contents

List of Figures vi

List of Tables vii

Abbreviations viii

Chapter 1: Introduction 1

A) The Origin of X-chromosome Inactivation 1

1. Sex Chromosome Evolution 1

2. Two Types of X-chromosome Inactivation Have Evolved 4

B) Molecular Biology of X-chromosome Inactivation 5

1. Initiation of X-chromosome Inactivation 6

2. Maintenance of XCI 10

C) Linking X-chromosome Inactivation to Cell Potency 12

1. X-chromosome Activity in Pluripotent Cells 12

2. Regulated *Xist* expression in Pluripotent Cells 13

D) X-chromosome Inactivation in the Preimplantation Female Mouse Embryo 15

1. The Xp acquires epigenetic markers of XCI during preimplantation development 17

2. Segregation of Cell Lineage in the ICM of the Blastocyst 17

Chapter 2: Imprinted XCI occurs in all cells of female blastocysts 20

A) Xp silencing is established in the ICM prior to epiblast specification 21

B) NANOG does not strictly denote X-chromosome activation 23

D) Materials and Methods 29

Chapter 3: Reactivation of Imprinted XCI in the ICM 34

A) Reactivation of the Xp occurs in the presence of Xi epigenetic modifications 34

B) Reactivation of Xp-linked genes occurs exclusively in the epiblast lineage 41

C) Chromosome-wide transcription occurs in the presence of *Xist* Coating 42

D) H3K4me2 overlaps the Xp EED domain 47

E) Conclusions 47

F) Materials and Methods 50

Chapter 4: Extinction of *Xist* coating has no effect on Xp genic reactivation 54

A) Increased NANOG dosage results in loss of Xi epigenetic markers of XCI 55

B) Ectopic loss of *Xist* coating has no effect on Xp reactivation kinetics 56

C) Maintenance of Imprinted XCI in the blastocysts 60

D) Conclusions 60

E) Materials and Methods 63

Chapter 5: Discussion 65

A) Preliminary results, *Xist* coating in Initiation of Random XCI 65

B) Future Directions 71

C) Concluding Remarks 75

C) Methods 78

Bibliography 80

List of Figures

Figure 1 The Xi repressive compartment model for XCI 9

Figure 2 Lineage specification in the ICM 19

Figure 3 X-linked gene expression during preimplantation development..... 22

Figure 4 Imprinted Xp silencing in the early stage blastocyst..... 24

Figure 5 NANOG does not denote X-chromosome Activation..... 26

Figure 6 Mid-stage ICMs exhibit increasing Xp expression 36

Figure 7 X-linked gene expression assayed by allele-specific RT-PCR 39

Figure 8 *Nanog* expression is associated with biallelic X-linked gene expression 43

Figure 9 Mid-stage ICMs exhibit transcription within the Xp-*Xist* domain. 44

Figure 10 Epigenetic marks associated with transcription overlap the Xp EED domain. 45

Figure 11 *Grb2* $^{-/-}$ ICM cells exhibit loss of *Xist* transcripts and EED on the Xp..... 57

Figure 12 Loss of *Xist* coating does not alter reactivation kinetics 58

Figure 13 *Grb2* $^{-/-}$ ICM nuclei maintain Xp-linked gene silencing through cell divisions..... 59

Figure 14 Characterization XCI-associated epigenetic marks in mid-stage blastocysts. 61

Figure 15 Epiblast cells exhibit Xi gene silencing in the absence of *Xist* coating..... 69

List of Tables

Table 1 Percentage of Monoallelic, Biallelic, and Nonscorable Nuclei Measured by RNA FISH 37

Table 2 Mean Percentage of Xp Expression As Measured Allele-Specific RT-PCR 40

Abbreviations

BSA	Bovine Serum Albumin
Cdx2	Caudal-type homeobox 2
ChIP	Chromatin Immunoprecipitation
ChIP-seq	Chromatin Immunoprecipitation Sequencing
CSK	Cytoskeletal Buffer
ES cells	Embryonic stem cells
EpiSCs	Epiblast stem cells
FGF	Fibroblast growth factor
Fgf4	Fibroblast growth factor-4
Fgfr2	Fibroblast growth factor receptor 2
FISH	Fluorescent *in situ* hybridization
Gata6	GATA-binding factor 6
GRO-seq	Global run-on sequencing
Grb2	Growth factor receptor-bound protein 2
H2AK119ub1	Ubiquitination of histone H2A at lysine 119
H3K4me2	Di-methylation of histone H3 at lysine 4
H3K9me3	Trimethylation of histone H3 at lysine 9
H3K27me3	Trimethylation of histone H3 at lysine 27
H4K20me1	Monomethylation of histone H4 at lysine 20
ICM	Inner cell mass
MSL	Male-specific lethal complex
MOF	Males absent on the first
MSCI	Meiotic sex chromosome inactivation (MSCI)
MAPK	Mitogen-activated protein kinase (MAPK)

Nanog	Nanog homeobox protein
Oct4	Octamer-binding transcription factor 4
PRC2	Polycomb Repressive Complex 2
PRC1	Polycomb Repressive Complex 1
PARs	Pseudoautosomal regions
RT-PCR	Reverse transcribed PCR
RNA-seq	RNA-sequencing
Sry	Sex determining region Y
Sox2	Sry-related HMG-box 2
Sox3	Sry-related HMG-box 3
SNPs	Single nucleotide polymorphisms
TSSs	Transcription Start Sites
TS cells	Trophoblast stem cells
XCI	X-chromosome Inactivation
Xi	Inactive X-chromosome
Xist	X-inactive specific transcript
Xm	Maternal X-chromosome
Xp	Paternal X-chromosome
WT	Wild type

Chapter 1: Introduction

A) The Origin of X-chromosome Inactivation

1. Sex Chromosome Evolution

Humans, like other mammals, are a diocecious species. That is, sex is determined by chromosome karyotype. Mammalian females have two X-chromosomes (XX), whereas males have one X- and one Y-chromosome (XY). The X- and Y-chromosomes are genetically distinct; however, DNA sequencing indicates that approximately 5% of their sequence is identical. In humans, these identical sequences, referred to as the pseudoautosomal regions (PARs), are grouped at the chromosome ends and undergo recombination during male meiosis. The presence of the PARs suggests that the X- and Y-chromosomes evolved from an identical origin, likely an ancestral autosome pair (Cooke et al., 1985; Rappold, 1993).

The human X-chromosome contains approximately 2,000 genes that code for proteins utilized in a variety of cellular processes. Contrarily, the human Y-chromosome is considerably degenerate, highly-repetitive, and low in gene density; the few Y-linked genes that have been retained code for proteins required for male sex determination, fertility, and fitness in male offspring (Graves, 2010). The retention of 'maleness genes' and the degeneration of Y-linked sequence suggest a mechanism that may explain the differentiation

of the sex chromosome from an identical ancestral autosome; likewise, the origins of X-Chromosome Inactivation (XCI) can also be traced to this mechanism.

Sequencing across mammalian species indicates that Y-linked genes arose from mutations in proto-X-linked genes that acquired male-specific functions. For example, the master controller of male sex determination the *Sex determining region Y* (*Sry*) gene can trace its origin to a mutation in the proto-*Sox3* gene, now X-linked. Over time, as additional Y-linked genes differentiated from their proto-X-linked counterparts, it became necessary to fix these genes on the Y-chromosome, preventing their shuffling to the X-chromosome. Linking 'maleness' genes to the Y-linked sex determination gene *Sry* also had the added bonus of ensuring that 100% of male offspring inherited alleles that were advantageous to males. In order to group Y-linked genes, recombination was progressively eliminated between the X- and Y-chromosomes. Comparative genomic mapping across monotremes, marsupials, and eutherians, has shown that the Y-chromosome accumulated regional, block-like inversions over evolutionary time, such that ninety-five percent of the human X- and Y-chromosome sequence do not undergo recombination in the male germline. This contrasts with larger regions of recombination found between the marsupial and monotremes X- and Y-chromosomes. Between identical chromosomes, homologous recombination is advantageous, maintaining genome integrity by repairing harmful mutations, shuffling alleles to preserve well-adapted haplotypes, and replacing ill-adapted haplotypes (Muller, 1964). While limiting recombination between the sex chromosomes was a necessity, it resulted in the accumulation of destructive mutations and the decay, disappearance of Y-linked sequence (Rice, 1994). The X-chromosomes, which undergo homologous recombination in the female

germline, have preserved nucleotide integrity and thus maintained ancestral gene content (Graves, 2010).

A consequence of X- and Y-chromosome differentiation is that most genes on the X-chromosome exist as a single copy. Ultimately, without compensatory mechanisms, protein production would be halved in males. Whereas haploinsufficiency of a single gene, depending on the gene, many not compromise the health of an organism, haploinsufficiency for most X-linked genes would disturb the balance of many gene expression networks, resulting in decreased fitness and mortality. To compensate for the decay of the Y-chromosome, the activity of X-linked genes, as compared to an autosome, is increased two-fold (Cheng and Disteche, 2006; Lin et al., 2007; Zhang and Oliver, 2007). An upregulation of X-linked genes is common to many species, but the mammalian mechanism is entirely unknown. In *Drosophila melanogaster*, expression from the single X-chromosome in males is upregulated two-fold, but no upregulation occurs in females (Kelley et al., 1995). In mammals and *Ceanorhabditis elegans* upregulation of the X-chromosome occurs in both sexes (Cheng and Disteche, 2006). In mammals, data suggests that a chromatin-modifying complex, similar to the MSL complex in *Drosophila melanogaster*, may have evolved to target X-linked sequences in general (Rea et al., 2007). For example, in mammalian cells with two active Xs—undifferentiated female embryonic stem (ES) cells—both X-chromosomes appear to be upregulated (Lin et al., 2007).

Increasing the number of RNA transcripts from the X-chromosomes replenishes protein levels in males, but it creates an excess of X-linked transcripts in females. Placental mammals (marsupials and eutherians) evolved a second compensatory mechanism termed X-chromosome inactivation (XCI) (Lyon, 1961). In any cell that has more than one X-

chromosome per diploid autosome set, the cell inhibits transcription from all but one X-chromosome. Generally, XCI is thought to occur exclusively in XX females rendering X-linked gene dosage equivalent between males and females. It is unknown if and how XCI and X-chromosome upregulation mechanisms interact to achieve overall dosage compensation.

2. Two Types of X-chromosome Inactivation Have Evolved

XCI is a developmentally regulated process. Female offspring inherit an active X-chromosome from both the maternal (Xm) and paternal (Xp) germline (Kalantry et al., 2009; Namekawa et al., 2010; Patrat et al., 2009). In humans, XCI is initiated at the 8-cell stage of preimplantation development (van den Berg et al., 2009). The choice to inactivate the Xm or the Xp is independent and random in each cell of the embryo. Once XCI is initiated, the inactive state of that X-chromosome is replicated through cell divisions so that XCI is fixed with the cell's heredity. Random XCI produces a mosaic of cells that express X-linked genes either from the Xm or the Xp (Moreira de Mello et al., 2010). In the embryo proper, random XCI is conserved in eutherian mammals. However, in all tissues of marsupials and extraembryonic tissues of some eutherian embryos, such as rodents and bovine, only the paternal X-chromosome is inactivated (Takagi, 1978; Takagi and Sasaki, 1975; West et al., 1977; Xue et al., 2002). This form of XCI is termed, imprinted.

The high degree of sequence homology between marsupials and eutherians (the marsupial X shares homology with two-thirds of the eutherian X and corresponds to an ancient conserved region) and observations of imprinted XCI in some eutherian tissues suggest that the two types of XCI may have arisen from a common mechanism (Deakin et al., 2009). However, models that explain XCI in eutherians utilize whole X-chromosome based

mechanisms. The mechanism of marsupial XCI is unknown, but many of the whole chromosome epigenetic features that are inherent to eutherian XCI are not present in marsupials. Marsupial XCI is also far less complete, implicating local regulatory mechanisms in genic silencing, which is consistent with comparative mapping studies that suggest sex chromosome evolution did not occur all at once (Lahn and Page, 1999). Given their similar origin, it may be that silencing mechanisms have been conserved throughout the evolution of XCI, but many researchers in field also argue that XCI in marsupials and eutherians could have evolved uniquely. Thus, imprinted and random XCI may have mechanistic differences. How the mechanisms of imprinted and random XCI resemble each other is currently a topic of much debate.

B) Molecular Biology of X-chromosome Inactivation

X-chromosomes are inherited by female offspring as transcriptionally active, undergo inactivation during early embryonic development, and then re-activate again in the germline. These faithful cycles of activation and inactivation indicate that the transcriptional status of the X-chromosome is regulated by epigenetic mechanisms, such that XCI requires heritable alterations to gene expression that are not implemented by changes to the DNA sequence. These mechanisms must explain how: (1) genetically identical chromosomes become stably differentiated from one another within the same nucleus and (2) how the inactivation state is faithfully maintained through cell divisions during the lifetime of the female. Based on these two requirements, XCI mechanisms have been divided into phases of initiation and maintenance.

1. Initiation of X-chromosome Inactivation

Mechanisms to explain how cells identify one X-chromosome among all the chromosomes in the genome to select for silencing are beyond the scope of the current knowledge of epigenetics. In addition, how embryonic cells inactivate X-chromosomes at random or distinguish parental origin is a poorly understood subject with much complexity. Parent-of-origin specific XCI is an example of genomic imprinting; other examples of imprinted gene expression can be found at domains of autosome-linked genes (Ferguson-Smith and Surani, 2001). Germline-derived epigenetic modifications are hypothesized to regulate parent-of-origin bias in X-chromosome activity. Data indicate that XpO mice are viable, and androgenetic embryos (XpXp) undergo random XCI in the extraembryonic tissues. Therefore, if an inactivating Xp imprint is deposited in the male germline, then it is reversible (Okamoto et al., 2000; Thornhill and Burgoyne, 1993). These data have led some to hypothesize that imprinting depends on marking the Xm for transcriptional activation. In support of this hypothesis, XmXm embryos do not undergo XCI (Goto and Takagi, 1998). De novo methylation during oocyte maturation is essential for setting maternal imprints, and germline specific knockouts of the de novo methyltransferases disrupt parentally biased gene expression within imprinted domains of autosomes (Kaneda et al., 2004). Conversely, allelic expression of X-linked genes is unchanged in these mutant embryos (Chiba et al., 2008). The X-chromosome may therefore be regulated in a manner that is distinct from traditional imprinting. Future studies may elucidate the mechanisms that determine which X-chromosome is chosen for silencing, but currently mechanisms of both imprinted and random XCI are unknown.

Initiation of XCI is marked by widespread repression of inactive-X (Xi) genes, yet one locus, the *X-inactive specific transcript (Xist)* gene, is uniquely upregulated from the Xi allele (Brown et al., 1991). The *Xist* gene codes for a 15kb processed but untranslated RNA molecule that is stabilized in the nucleus and localizes in numerous copies to the Xi; this localization in cis is commonly referred to as *Xist* coating (Figure 1A) (Brockdorff et al., 1992; Clemson et al., 1996). *Xist* coating represents the earliest known event in XCI, occurring coincident with gene silencing, and loss-of-function mutations demonstrate that *Xist* is absolutely required for XCI (Kay et al., 1993). Its early localization has led to the prevailing opinion that *Xist* is the master regulator of XCI, and models have implicated *Xist* coating in regulating all molecular events in the XCI process. The exact role of *Xist* is yet undetermined, and the molecular events that lead to initiation of X-linked gene silencing are still being unraveled.

Within the nucleus, each chromosome is localized to a discrete domain, called a chromosome territory. The chromosome territory of the Xi is distinct from its active counterpart and is organized into a nuclear domain, referred to as the Xi silent repressive compartment that is globally depleted for RNA polymerase II (Figure 1B and C) (Chaumeil et al., 2006). Microscopically, the silent Xi compartment is coated by *Xist* transcripts and *Xist* coating is likely responsible for folding the chromosome into its characteristic topology (Splinter et al., 2011). X-linked genes, irrespective of their future expression status, are initially positioned at the exterior edge of the Xi domain, which is in contact with the transcriptional machinery; upon silencing the genic sequences are drawn into the interior of the silent Xi compartment and encompassed by *Xist* coating. Relocation of X-linked genes

into the silent compartment is thought to initiate silencing by preventing access of the transcriptional machinery to Xi genes (Figure 1C).

This inside-repressed/exterior-active chromosome territory model is based primarily on *fluorescence in situ hybridization* (FISH) studies interrogating the position of a small number of X-linked genes in relation to the *Xist* domain. The chromosome territory model may, therefore, be an oversimplification of Xi topology. The model also assumes that transcriptional machinery cannot access the interior of the Xi territory. Within autosomal chromosome territories, interior positions are correlated with gene repression but are not repressive for the transcriptional machinery (Morey et al., 2009; Schneider and Grosschedl, 2007). In fact, RNAPII and chromatin remodelers are capable of accessing genes, suggesting that chromosome territories may be more porous than the Xi repressive compartment model accounts. Localization exterior to chromosome territories is also not sufficient to induce autosomal gene expression. Currently, it is unknown if chromosome topology actively participates in transcriptional repression or is a reflection of transcriptional repression.

There is data to argue against *Xist* RNA dependent chromosome folding as the mechanisms of Xi transcriptional repression. For example, two recent reports suggest disconnect between the exclusion of RNA Polymerase II from within the Xi territory and *Xist* coating, indicating that (1) RNA Polymerase II can be depleted from the imprinted Xp in the absence of *Xist* transcripts and that (2) inducing *Xist* expression does not result in formation of a RNA Pol II-depleted domain (Namekawa et al., 2010; Thorogood and Brown, 2010). Female embryos inheriting a null mutation for *Xist* on the paternal (Xp) X-chromosome also transiently initiate silencing of many Xp-linked genes (Kalantry et al., 2009). Together,

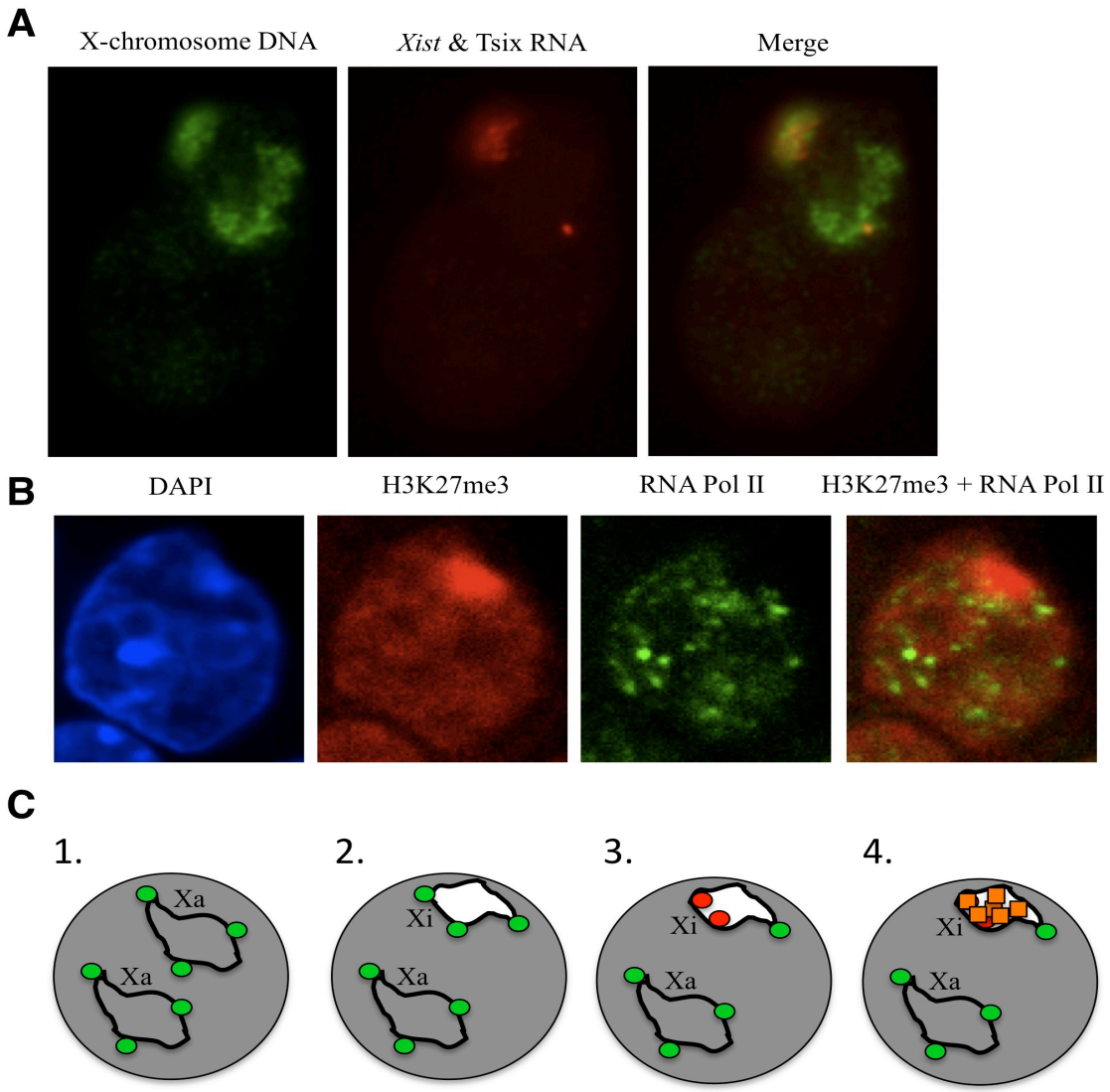

Figure 1 The Xi repressive compartment model for XCI.

(A) X-chromosomes are labeled by DNA FISH with an X-chromosome paint (green, first panel). RNA FISH detects *Xist* transcripts (red, middle panel) coating the Xi. The Xi is densely packaged relative to the more open, diffuse Xa. **(B)** A domain of H3K27me3 immunostaining (red, second panel) marks the Xi. Within the Xi H3K27me3 domain, RNA Polymerase II (green, third panel) is depleted (merge), forming what is referred to as the Xi silent repressive compartment. **(C)** (1) Prior to the onset of XCI, both X-chromosomes are active and the chromosome territories are identical. (2) Once an X-chromosome is chosen for silencing, *Xist* transcripts coat and RNA Polymerase is excluded from within the Xi terrority. This forms the silent repressive compartment (white). All genes are active and are located on the exterior (green). (3) When X-linked genes silencing is initiated, genes are re-positioned into the interior of the compartment (red), such that they no longer make contact with transcriptional machinery. (4) Histone modifications and other epigenetic modifying proteins form a domain over the Xi silent repressive compartment (orange blocks) 'locking' the Xi into its silent state.

these data imply that *Xist* coating may not be the single initiator of XCI, and yet undiscovered initiators of Xi gene silencing may exist. Thus, initiation of the XCI process may be more complicated than current models predict.

2. Maintenance of XCI

Once Xi gene silencing is initiated, maintenance mechanisms ensure that replicated copies of the Xi are inherited as inactive during rounds of cell division. The Xi exhibits many features characteristic of heterochromatin: it replicates late, is localized to the nuclear periphery, and exhibits a deficit of chromatin modifications associated with transcription, such as histone H4 hyperacetylation. Contrasting the general depletion of components associated with transcription, chromatin at Xi genes is enriched relative to the rest of the genome for chromatin modifications associated with gene repression, such as trimethylation of histone H3 at lysine 27 (H3K27me3), mono-ubiquitination of histone H2A at lysine 119 (H2AK119ub1), trimethylation of histone H3 at lysine 9 (H3K9me3), and monomethylation of histone H4 at lysine 20 (H4K20me1) (de Napoles et al., 2004; Mermoud et al., 2002; Plath et al., 2004; Wang et al., 2001). The molecular basis for these chromatin modifications in maintaining X-linked gene silencing has yet to be determined; these modifications may condense the chromatin or cooperate with unknown initiating factors to block the transcriptional machinery. Chromatin immunoprecipitation (ChIP) experiments have provided some functional insight. For example, genome-wide H3K27me3 is largely restricted to repressed CpG-rich promoters, (Ku et al., 2008; Mendenhall et al., 2010) yet H3K27me3 is also dispersed within Xi gene bodies (Marks et al., 2009).

Methylation of CpG islands within X-linked promoters also has a critical role in stabilizing random XCI, but DNA methylation does not appear to play an essential role in

extraembryonic tissues (Sado et al., 2000). Recently, the cohensin-like, hinge domain containing protein SMCHD1 has been implicated in recruitment of DNA methyltransfersases to the Xi (Blewitt et al., 2008). The chromatin remodeler ATRX and the histone variant macroH2A also exhibit chromosome-wide Xi enrichment (Garrick et al., 2006; Mietton et al., 2009). Protein complexes utilized in DNA repair, such as ATM and BRCA1, and nuclear architecture, such as SATB1, are also associated with the Xi (Agrelo et al., 2009; Garrick et al., 2006; Ouyang et al., 2005; Vincent-Salomon et al., 2007). The involvement of replication and nuclear organization machinery denotes that, in addition to the preservation of gene expression patterns, conservation of genome stability is also essential for stable XCI.

In contrast to the rather elusive role of *Xist* in initiation of XCI, *Xist* coating has a defined role in maintenance of XCI. Localization of *Xist* RNA is not required for long-term maintenance of XCI, but coating of the Xi by *Xist* is necessary and sufficient to establish Xi heterochromatin (Wutz and Jaenisch, 2000). H3K27me3, which is the first chromatin modification deposited on the Xi, is catalyzed by EZH2 of the Polycomb Repressive Complex 2 (PRC2) (Mak et al., 2004). Small RNAs have been shown to be co-factors for recruitment of the PRC2 complex to genome-wide targets, and *Xist* and *Hotair*, a long non-coding RNA that regulates *HOX* gene expression, are co-factors for PRC2 recruitment (Zhao et al., 2010). Female embryos lacking either *Xist* RNA or PRC2 components exhibit complete loss of Xi epigenetic markers, including H2A119ub1, H4K20me3, and macroH2A suggesting that *Xist* is also involved in recruitment of these complexes to the Xi, either independently or via PRC2 (Kalantry et al., 2006).

The Xi is remarkably stable, owing to a cascade of epigenetic events that actively maintain the inactive state. No one of these factors or epigenetic modifications has been

shown to be individually required for the maintenance of XCI and rarely are all of these factors/modifications detected simultaneously on the Xi. This implies that redundant mechanisms or additional not-yet described factors are required for stable Xi gene silencing. Many of these features are regulated during the cell cycle, but some Xi chromatin signatures do persist through mitosis, implying active participation in the epigenetic transmission of XCI (Chaumeil et al., 2002; Mak et al., 2002).

C) Linking X-chromosome Inactivation to Cell Potency

1. X-chromosome Activity in Pluripotent Cells

The potency of a cell defines the cell's potential to differentiate into multiple cell types. Totipotent cells, such as germ cells, are able give rise to all the cells of the embryo, including extraembryonic tissues. Pluripotent cells are slightly more restricted having the ability to differentiate into the three lineages (endoderm, mesoderm, ectoderm) that develop the embryo but cannot differentiate into extraembryonic tissues. XCI is required in female cells to equalize X-linked gene expression between the sexes. Interestingly, female totipotent and pluripotent cells disobey this requirement, exhibiting two active X-chromosomes (Epstein, 1969; Tam et al., 1994). An association between potency and the mechanisms that regulate X-linked gene activity has long been hypothesized. In further development of this association, reprogramming of somatic cells results in reactivation of the somatically silent Xi (Takagi et al., 1983). Reciprocally, exit from pluripotency by differentiation induces initiation of random XCI in ES cells.

2. Regulated *Xist* expression in Pluripotent Cells

The pluripotent cells of the mammalian embryo are specified in the Inner Cell Mass (ICM) of the developing blastocyst. *In vivo*, the ICM matures into the pluripotent epiblast, the founder tissue of the embryo. *In vitro,* ICMs can be maintained in culture to derive ES cells that retain pluripotency along with the unlimited capacity to self-renew in culture (Smith, 2001). Octamer-binding transcription factor 4 (OCT4), SRY (Sex-determining region Y)-box2 (SOX2), and Nanog homeobox (NANOG) function as master regulators of a highly integrated protein-protein interaction landscape that is necessary to establish and sustain the expression of thousands of genes required for pluripotency. Moreover, these transcription factors are also required for proper differentiation (Boyer et al., 2005). NANOG, OCT4, and SOX2 co-precipitate with chromatin from a number of repressed genes in ES cells, termed bivalent domains, and with the help of chromatin modifying proteins, such as PRC2 and PRC1, have been shown to poise cells for differentiation (Bernstein et al., 2006).

The active X-chromosomes in female ES cells are characterized by low-levels of *Xist* expression, and coating by *Xist* is blocked by strong transcriptional repression of *Xist* via reduced levels of the basal transcriptional machinery associated with the *Xist* promoter (Navarro et al., 2005). Testing the relevance of pluripotency in regulated XCI has long been complicated because knockdown of factors required for pluripotency forces differentiation of female ES cells, triggering XCI. Recently, Navarro and Avner circumvented this problem by utilizing male ES cells, which normally never undergo XCI. These authors first showed that *Xist* is a direct target of OCT4, SOX2, and NANOG in ES cells. Then, utilizing NANOG-depleted male ES cells these authors implicate NANOG in

regulating *Xist* repression, as loss of NANOG resulted in rapid transcriptional upregulation of *Xist*. In separate experiments, genetic invalidation of OCT4 resulted in drastic loss of OCT4, SOX2, and NANOG at *Xist* intron 1 that was accompanied by *Xis*t coating of the single X-chromosome. Based on these data, it was concluded that the activity status of X-chromosomes in undifferentiated female cells depends on the ability of OCT4, SOX2, and NANOG to regulated *Xist* transcription and prevent *Xist* coating (Navarro et al., 2008). Similar to other repressed targets in ES cells, the pluripotency-associated transcription factors may also coordinate initiation of random XCI by regulating the upregulation of *Xist* expression upon differentiation (Navarro and Avner, 2009).

These data indicate a coupling of the pluripotency-associated transcription factors in at least one aspect of XCI, but the mechanism underlying *Xist* repression remain to be elucidated. For example, additional experiments are required to determine how binding of these factors within the first intron of *Xist* influences transcription. These results have also not been validated in mouse embryos. This model also assumes that all mechanistic aspects of XCI depend on *Xist* RNA. If in fact Xi gene silencing can occur in the absence of *Xist* coating, as data analyzing imprinted XCI suggests, then additional experiments are needed to understand how these *Xist*-independent mechanisms may be regulated by cell potency.

In contrast to mouse ES cells X-chromosome activity in female human ES cell lines is dynamic. Pluripotent human ES cells exhibit three states of XCI: class I cells carry two active X-chromosomes; class II cells exhibit XCI and the Xi is coated by *Xist*; and, class III cells exhibit an Xi that is not coated by *Xist* (Hall et al., 2008). These data might suggest that a lack of XCI is not an exclusive characteristic of pluripotency. Conversely, class I cells may represent the natural condition of XCI *in vivo*. Class II and class III cells may be

epigenetically unstable having progressed beyond naive pluripotency to a pre-differentiated condition. It is thought that these cells are anomalies of sub-standard *in vitro* culture conditions (Lengner et al., 2010), but recent analysis of at least one X-linked gene, *Atrx*, has suggested that the patterns of XCI evident in human ES cells may recapitulate those of human ICMs (Okamoto et al., 2011). Further analysis in human embryos will likely resolve some of this controversy. Even so, the current data indicate that relative *Xist* expression levels are not correlated with levels of *Oct4*, *Nanog*, and *Sox2* transcripts in early passage human ES cell lines. These results were supported by simultaneous appearance of *Xist* coating and OCT4, NANOG, and SOX2 protein by immunostaining (Dvash et al., 2010). From these data, it may be hypothesized that factors in addition to OCT4, SOX2, and NANOG determine X-chromosome activity in pluripotent cells, either via *Xist* or by alternative mechanisms.

D) X-chromosome Inactivation in the Preimplantation Female Mouse Embryo

Preimplantation development is characterized by events that prepare the embryo for uterine implantation and support embryonic development. These events occur during discrete phases of fertilization, cleavage, and blastocyst formation. A variety of epigenetic mechanisms underlie the transformation of the embryonic genome from totipotent to the more committed blastocyst, and imprinted X-chromosome inactivation can be considered a case study of the epigenetic regulation during preimplantation development (Corry et al., 2009).

After fertilization the epigenetic states of the oocyte-derived maternal genome and sperm-derived paternal genomes must be reset. These epigenetic events are strictly coordinated to allow for timely zygotic gene expression (Nothias et al., 1995). In the newly

formed 1-cell zygote, both maternal and paternal genomes are highly condensed and transcriptionally inactive; the maternal and paternal genomes are also individually packaged into separate membranes forming the maternal and paternal pronuclei. Consistent with transcriptional repression both maternal and paternal genomes are highly methylated prior to fertilization. After fertilization, the paternal genome undergoes active DNA demethylation, without DNA replication, that is tightly linked to male pronucleus formation (Mayer et al., 2000; Oswald et al., 2000). Interestingly, there is protection against active DNA de methylation in the female pronucleus, as well as autosomal imprinted loci in the male pronucleus (Nakamura et al., 2007). Transcriptional activity is first detected in the 1-cell zygote when the two genomes are still individually packaged in the pronuclei. This first wave of zygotic genome activation occurs earlier and at increased levels in the male pronucleus. It is possible that the differential DNA methylation and transcriptional activation between the maternal and paternal genomes at the 1-cell stage may drive differential treatment of the X-chromosomes in imprinted XCI.

The first cleavage division is characterized by synkaryogamy, the breakdown of pronuclear membranes and fusion of maternal and paternal genomes. At the 2-cell stage, zygotic genome activation is complete and both X-chromosomes are active in the 2-cell stage embryo (Kalantry et al., 2009; Namekawa et al., 2010; Patrat et al., 2009). The Xm retains its activity throughout preimplantation development. The Xp, conversely, exhibits gradual accumulation of epigenetic modifications associated with heterochromatin. The accumulation on the Xp of repressive marks contrasts with the gradual, passive genome-wide DNA de methylation that is inherent to the epigenetic profile necessary for differentiation

into trophectoderm, primitive endoderm, and epiblast at the blastocyst stage (Morgan et al., 2005).

1. The Xp acquires epigenetic markers of XCI during preimplantation development

Initiation of imprinted XCI is first observed by the microscopically detectable depletion of RNA Polymerase II from the Xi territory at the 4-cell stage, which coincides with coating of the chromosome by *Xist*. By the 8-cell stage, *Xist* coating is apparent on the Xp in all nuclei. At this time, Xp-linked gene silencing is initiated, with some nuclei of the 8-cell stage embryo showing silencing of Xi genes. *Xist* coating recruits PRC2, and by blastocyst stage, there is an observable H3K27me3 enrichment domain that colocalizes with the Xp in all nuclei (Mak et al., 2004; Okamoto et al., 2004).

2. Segregation of Cell Lineage in the ICM of the Blastocyst

The blastocyst stage of preimplantation development is not discrete; in fact, over approximately 36 hours of development, the mouse blastocyst undergoes dynamic differentiation. The early-stage blastocyst (~32 cells) is divided into two cell populations, trophectoderm and ICM. The trophectoderm is the progenitor of the placenta. Trophectoderm cells line the exterior of the blastocyst and become distinguished by expression of *Cdx2* and repression of pluripotency-associated transcription factors *Oct4* and *Sox2*. The ICM reciprocally expresses *Oct4* and *Sox2* (Dietrich and Hiiragi, 2007). As the blastocyst expands, the ICM segregates into two populations of cells, primitive endoderm and epiblast that exhibit expression of lineage specific transcription factors *Gata6* and *Nanog,* respectively (Figure 2A). At the mid-stage (~32 to 64 cells) of blastocyst development, primitive endoderm and epiblast cells are randomly distributed within the ICM; however, by the late (greater than 64 cells) blastocyst stage, the endodermal lineages have

migrated to the exterior edge of the ICM and have upregulated *Gata6* (Figure 2A). The epiblast cells at this stage have high levels of *Nanog* expression (Plusa et al., 2008). The separation of primitive endoderm and epiblast cells in the ICM is thought to be directed by FGF signaling, and mutations in components of FGF signaling including *Fgf4*, *Fgfr2,* and *Grb2* results in early post-implantation lethality due to lack of primitive endoderm development (Figure 2B) (Lanner and Rossant, 2010; Yamanaka et al., 2010).

Given the presence of Xi epigenetic markers on the Xp in all cells, current models predict that all cells of the blastocyst establish imprinted XCI (Mak et al., 2004; Okamoto et al., 2004). In the following chapters, we provide definitive evidence, utilizing X-linked gene silencing, that imprinted XCI is established in all cells of the preimplantation embryo, supporting the current model. Imprinted XCI is thought to persist in the progenitor cells that will give rise to the extraembryonic tissues. Based on data from ES cells showing that OCT4, SOX2, and NANOG can repress *Xist* expression, upregulation of *Nanog* and subsequent loss of *Xist* coating in the epiblast cells of the late-stage ICM is thought to trigger reactivation of the imprinted Xp (Navarro and Avner, 2009). The result is that both X-chromosomes are active in the epiblast, and initiate subsequent random XCI upon gastrulation. Here, we examine the kinetics of reactivation in the ICM and in doing so, we hypothesize a new model for X-chromosome reprogramming and provide new insight into the mechanism of X-linked gene silencing.

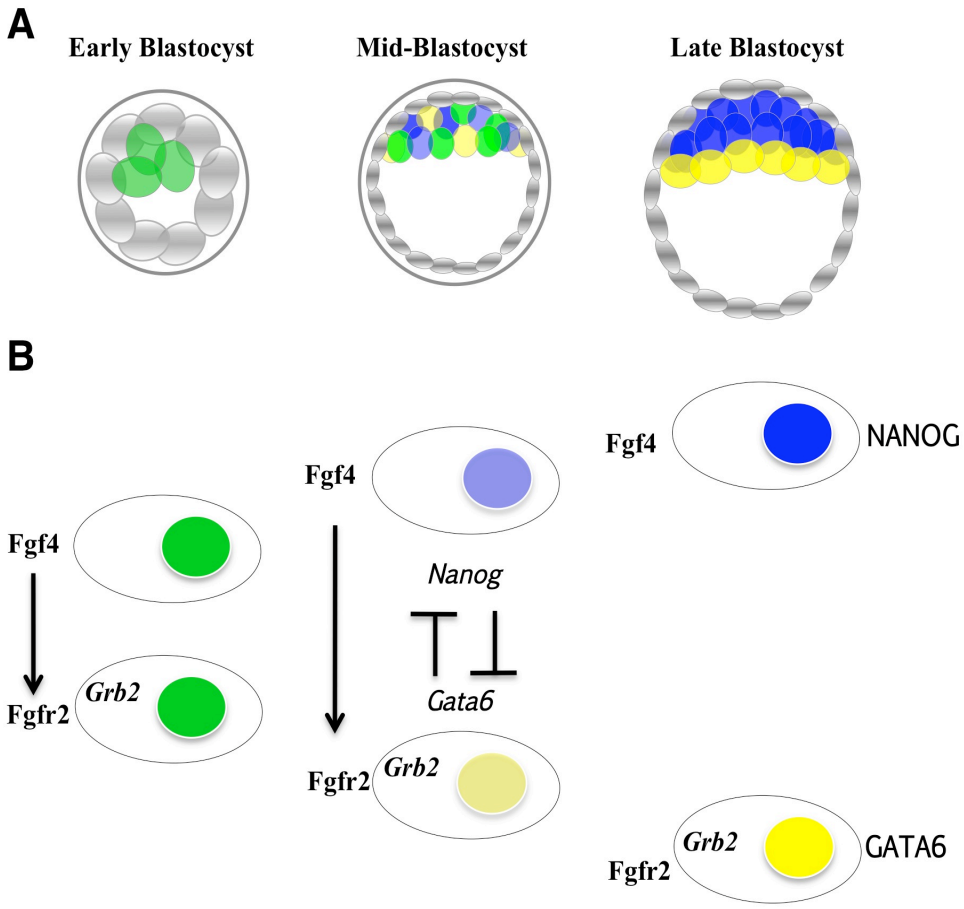

Figure 2 Lineage specification in the ICM.

(A) The ICM in early blastocysts consists of uncommitted cells (green) expressing both *Gata6* and *Nanog*. As the blastocyst develops, ICM cells begin to upregulated expression of either *Nanog* (blue) or *Gata6* (yellow). At late blastocyst stage, upregulation of *Nanog* and *Gata6* is complete such that cell fate is determined. **(B)** In early ICMs, cells exhibit variable levels of *Fgf4* and *Fgfr2* expression. The variability in these levels is enhanced as the ICM develops. Cells (yellow) exposed to high Fgf4 upregulate *Gata6*, which in turn results in down-regulation of *Nanog* expression. Where Fgf4 signaling is low (blue), *Nanog* expression is upregulated and *Gata6* is eventually repressed.

Chapter 2: Imprinted XCI occurs in all cells of female blastocysts

Previous analyses of X-linked gene expression quantified total mRNA by reverse-transcribed PCR (RT-PCR) in whole preimplantation embryos (Huynh and Lee, 2003; Okamoto et al., 2004; Ouyang et al., 2005; Singer-Sam et al., 1992). These results indicated that Xp-linked genes were expressed from the 2-cell to the 8-cell stage. At the 8-cell stage, the first Xp repression is detected (Kay et al., 1993). Utilizing RNA FISH, which detects gene activity with single-cell resolution, these results were corroborated; however, Xp silencing is heterogeneous in preimplantation embryos, with many nuclei having two-active X-chromosomes through the blastocysts stage (Figure 3B). One other group has independently reproduced these results (Patrat et al., 2009). All of these experiments have been performed on whole embryos. Here, we re-examined X-linked gene expression considering that the embryo contains two populations of cells: trophectoderm and ICM (Chazaud et al., 2006). We were especially curious about transcriptional status of the Xp in the ICM, which represents a minority of total cells in the mature blastocyst (approximately 10%). At stages of ICM development, ICM cells express pluripotency markers *Oct4, Sox2*, and *Nanog*. We reasoned that the presence of OCT4, SOX2, and NANOG prevents ICM cells from fully establishing imprinted XCI, contributing to the reported incomplete Xp silencing in whole embryos.

A) Xp silencing is established in the ICM prior to epiblast specification

To determine if all cells of the preimplantation stage embryo exhibit imprinted XCI, we analyzed transcription of X-linked genes by RNA fluorescent *in-situ* hybridization (RNA FISH). RNA FISH detects nascent transcripts at the origin of transcription. We analyzed ICMs isolated by immunosurgery (Solter and Knowles, 1975) from early-stage (~32 cell stage embryo) blastocysts .

Early-stage blastocysts were chosen for analysis because cell lineage in ICMs has not been specified; the early-stage ICM consists of a homogenous population of uncommitted cells (Plusa et al., 2008). We assayed five X-linked genes (*Rnf12, Atp7a, Abcb7, Ube1x,* and *Mecp2*) that are expressed at robust levels during preimplantation development (Kalantry et al., 2009; Patrat et al., 2009). RNA FISH had previously been used to analyze these five X-linked genes in whole embryos (Kalantry et al., 2009; Patrat et al., 2009). We assayed expression of the five X-linked genes together with *Xist* RNA, which is known to coat the Xp in all nuclei (Mak et al., 2004). If the Xp-allele of the five genes assayed is silenced, RNA FISH will yield a single monoallelic gene signal indicative of transcription from the Xm. In contrast, if the Xp-linked gene is not silenced, our assay will detect gene expression from both X-chromosomes (biallelic), and of the two RNA FISH signals will colocalize with the *Xist* domain. As a positive control, we measured expression of *Smcx*, a gene known to escape XCI during preimplantation development (Agulnik et al., 1994; Patrat et al., 2009).

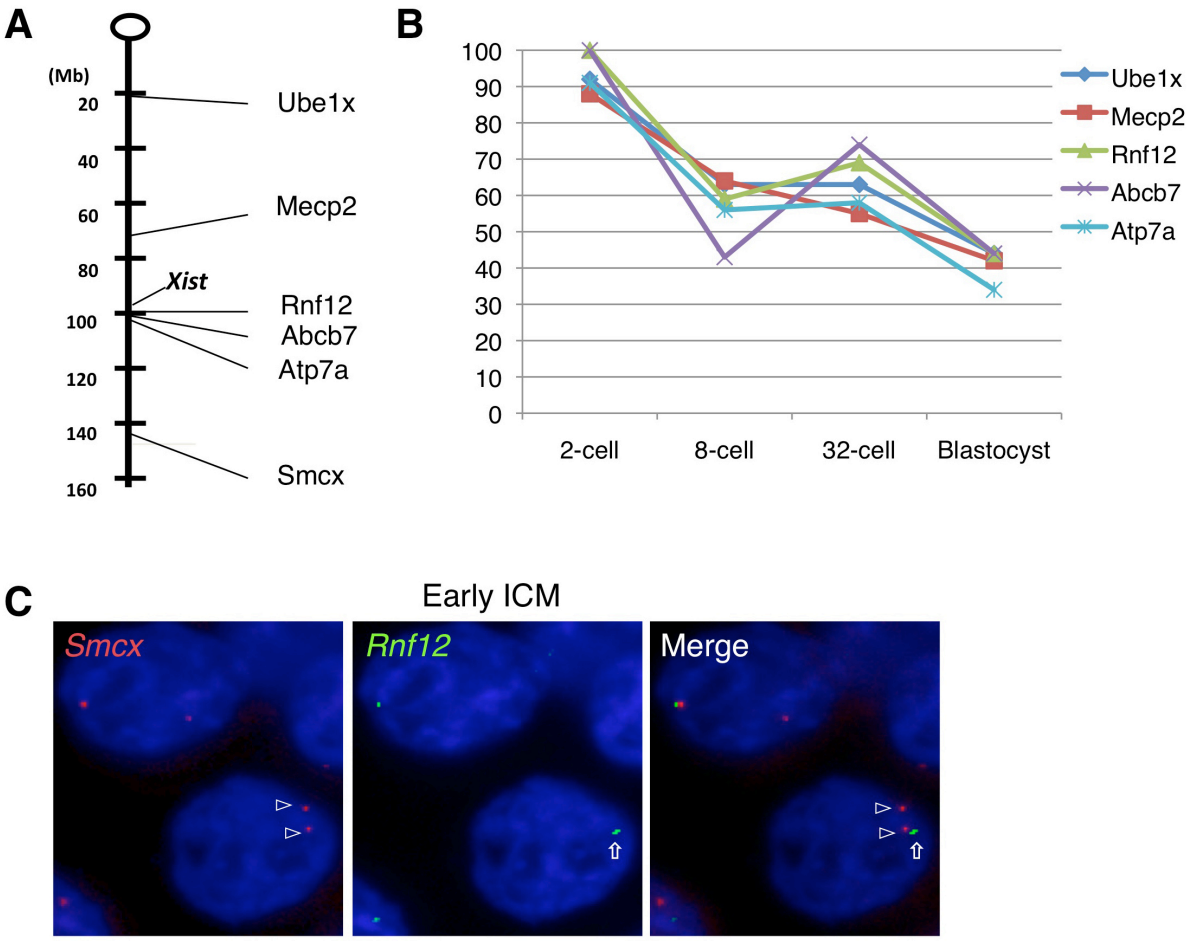

Figure 3 Transcription of X-linked genes during preimplantation development.

(A) The positions of the five X-linked genes analyzed by RNA FISH are graphically represented on the X-chromosome. Mb = megabase (B) For each X-linked gene, the kinetics of silencing during preimplantation development is graphed as a percentage of biallelic nuclei per total nuclei. (C) In early ICMs, RNA FISH is capable of detecting biallelism and monoallelism in the same nuclei (merge), which is indicated by detection of *Smcx* (red) and *Rnf12* (green) primary transcripts. Arrowheads mark biallelic expression of *Smcx*, an X-linked gene that escapes imprinted XCI (first panel). In contrast, a single arrowhead demarks monoallelic expression of *Rnf12* (middle panel).

As expected, *Smcx* exhibited 97% biallelic expression in early ICMs, demonstrating that our assay is capable of detecting X-linked gene transcription from the Xp (Figure 3C). In contrast, *Rnf12, Atp7a, Abcb7, Ube1x,* and *Mecp2* demonstrated an average low level of biallelism ranging between 5% and 23% of cells per ICM (Figure 4A and B). The degree of silencing depended on the gene assayed. For example, *Mecp2* had been reported to escape imprinted XCI, but we detected the average number of biallelic nuclei to be 18% of total nuclei examined (Patrat et al., 2009) *Rnf12*, *Atp7a*, and *Abcb7* exhibited efficient silencing with less than 10% biallelic nuclei. For all genes analyzed, the low level of biallelism in early ICMs was comparable to the level of biallelism found in the trophectoderm (Figure 4B). For *Rnf12*, *Atp7a*, *Abcb7,* and *Ube1x* a number of individual ICMs exhibited exclusive monoallelic X-linked gene expression in every nucleus, arguing against the possibility that a subset of ICM nuclei never undergo Xp silencing. Together, these data illustrate that the majority of nuclei exhibit an inactive Xp, thus the Xp undergoes imprinted XCI in the preimplantation embryo prior to specification of the embryonic lineage.

B) NANOG does not strictly denote X-chromosome activation

The finding that the *Xist* gene is a direct target of OCT4, SOX2, and NANOG suggests that these transcription factors are directly responsible for regulating X-chromosome activity. It has been proposed that *Xist* expression and as a by-product X-chromosome activity, is regulated by these transcription factors (Navarro and Avner, 2009). OCT4 and SOX2 are maternally supplied in the oocyte and exhibit widespread zygotic expression and protein localization patterns during preimplantation development. In contrast, NANOG is not maternally supplied; its zygotic expression is first detected at the 8-cell stage.

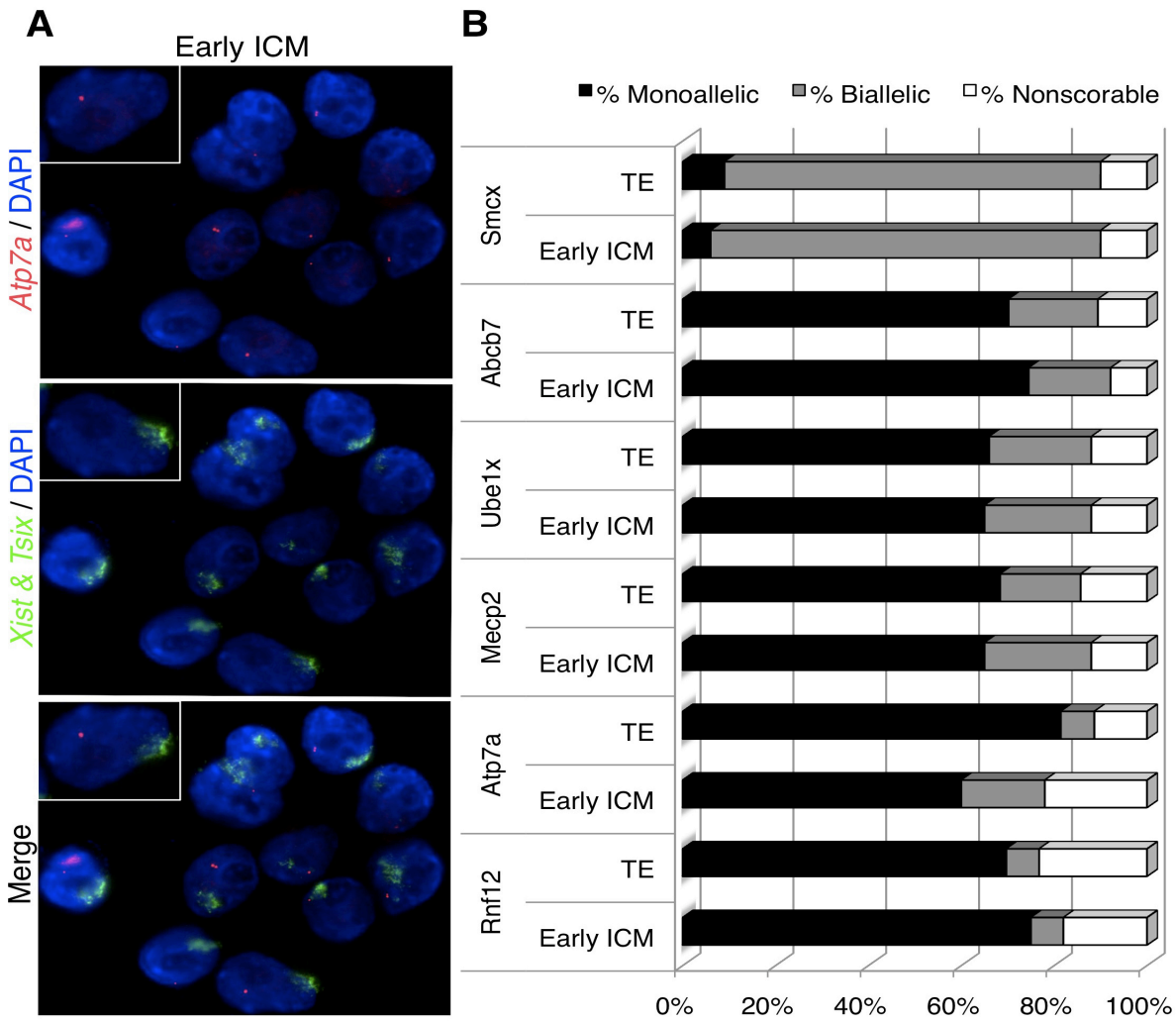

Figure 4 Imprinted Xp silencing in the early stage blastocyst.

(A) A representative ICM assayed for *Atp7a* (red, top panel) and *Xist/Tsix* (green, middle panel) by RNA FISH. The *Xist* probe detects *Xist* RNA and the anti-sense transcript *Tsix*. *Xist* marks the Xp as a cloud at this stage. In ICMs, *Tsix* is detected in some nuclei as a pinpoint signal from the Xm (Lee et al., 1999). In the merge image, all nuclei exhibit monoallelic *Atp7a* expression, localized away from the Xp-*Xist* coat (green domains). A single nucleus is highlighted in the right corner of each image. (B) Distributions of monoallelic (black), biallelic (grey), and nonscorable (white) nuclei are presented as average percentage of total nuclei per early ICM or trophectoderm. The distribution indicates that early ICMs exhibit a similar degree of monoallelic X-linked gene expression as the trophectoderm.

preponderant role in regulating *Xist* expression. It was also reported that NANOG positive cells in the early-stage blastocyst exhibited an Xp that did not have *Xist* coating(Mak et al., 2004).

The levels of NANOG vary in individual cells of undifferentiated ES cells and ICMs of mature blastocysts (Plusa et al., 2008). Given its role as a rheostat in regulating the achievement of ground-state pluripotency, we wondered if the levels of NANOG confer X-chromosome activity in the preimplantation embryo (Silva et al., 2009). Our immunostaining showed both strong and moderate NANOG staining in early-stage blastocysts. Importantly, high levels of NANOG colocalized with CDX2 (Figure 5A). Since CDX2 is a marker of extraembryonic cells, the colocalization of CDX2 and NANOG suggest that the presence of NANOG in early ICM nuclei is not indicative of epiblast specification, which is consistent with previous reports (Plusa et al., 2008). Connecting lineage specification to XCI, the colocalization of these markers makes it is also unlikely that NANOG denotes *Xist* repression.

As the blastocyst matures NANOG becomes restricted to the epiblast cells (Plusa et al., 2008). We reasoned that *Nanog* transcription is tightly regulated during blastocyst development, such that in contrast to protein localization *Nanog* transcripts may be detected only in cells that will retain NANOG at later stages. We performed RNA FISH with a probe that detects *Nanog* nascent transcripts. We examined early ICMs to determine if the few cells with an active Xp were exhibiting on-going *Nanog* expression. We found there was no association between Xp activation and Nanog expression (Figure 5B). The combination of our RNA FISH and immunostaining data argue that *Nanog* expression and NANOG localization are not markers of X-chromosome activation in the early stage blastocyst.

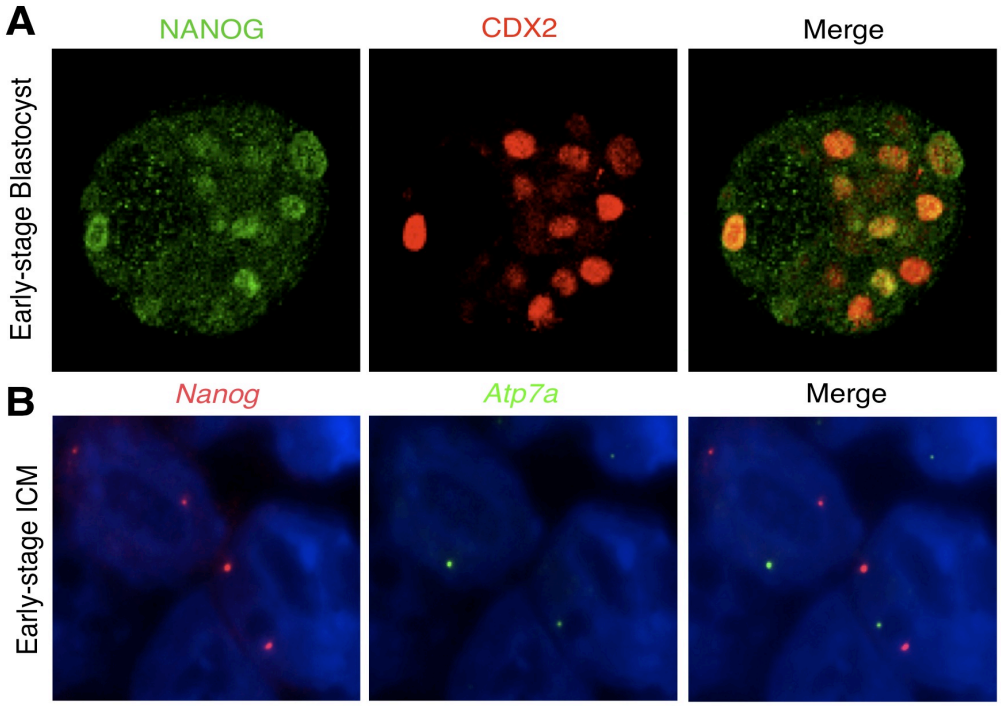

Figure 5 NANOG does not denote X-chromosome Activation.

(A) Early-stage blastocysts were immunostained for NANOG (green) and CDX2 (red), which is a marker of trophectoderm nuclei. Both lineage markers are present at high and low levels throughout the embryo, and some nuclei contain high levels of both NANOG and CDX2 (yellow, merge). (B) *Nanog* and *Atp7a* nascent transcripts are detected by RNA FISH in early-stage ICM nuclei. We see that in *Nanog* positive nuclei of early-stage ICM the Xp is silent, determined by monoallelic *Atp7a* expression.

C) Conclusions

Based on a genome-wide analysis of chromatin architecture in ES cells, pluripotent cells are defined by an open chromatin landscape, devoid of compaction. 8-cell stage mouse embryos have chromatin distributions similar to ES cell chromatin profiles, with an extended meshwork of loosely packaged chromatin, consistent with the embryo's uncommitted potential (Ahmed et al., 2010). This chromatin profile would appear non-conducive to initiation of XCI in that the Xi is characterized by chromatin compaction.

We utilized X-linked gene expression as the definitive marker of established XCI. Our data indicate that Xp-linked gene silencing is uniformly initiated in the early-stage blastocyst, such that ICMs and trophectoderm exhibit similar profiles of biallelic gene expression. These data confirm that, in the preimplantation mouse embryo, (1) all cells initiate imprinted XCI, (2) extraembryonic cells maintain imprinted XCI, and (3) epiblast-specified cells reprogram imprinted XCI, such that random XCI can be initiated at gastrulation.

Our data clearly show that preimplantation mouse embryos violate the rule of X-chromosome activation in female uncommitted cells. Mice are the primary organisms used in studies of XCI, but limited data indicate that other mammals also undergo XCI during preimplantation development. In bovine embryos, XCI is imprinted and the kinetics of XCI in bovine is very similar to mouse (De La Fuente et al., 1999). In rabbit embryos, XCI is delayed relative to mouse but analysis of one X-linked gene, *Hprt*, suggests robust Xi silencing has occurred by blastocyst stage. Significantly, the Xi is not reactivated in mature rabbit ICM cells, irrespective of the presence of OCT4, SOX2, and NANOG. Conversely,

human preimplantation embryos do not initiate Xi gene silencing, but *Xist* transcripts associated with X-chromosomes in nuclei of mature ICMs (Okamoto et al., 2011). XCI mechanisms are therefore highly diverse in early embryos and no clear association between cell potency and X-chromosome activity can be made.

Why do all cells of the mouse preimplantation embryo undergo imprinted XCI? One possible explanation is that XCI may be driven by the need of the preimplantation embryo to establish dosage compensation before trophectodermal lineage commitment. During mouse development, the trophectoderm is the first lineage specified and the majority of cells in the blastocyst are committed to the trophectoderm lineage. Trophectoderm specification occurs at compaction in the 32 cell stage mouse embryos and irreversible commitment is established by the mid-stage of blastocyst development (Dietrich and Hiiragi, 2007; Strumpf et al., 2005). Commitment of cells to trophectoderm is directed by *Cdx2*-dependent repression of *Oct4* expression (Niwa et al., 2005). Interestingly, bovine trophectoderm co-expresses *Oct4* and *Cdx2* and lineage commitment is delayed relative to mouse (Cauffman et al., 2005; Kobolak et al., 2009). Species-specific variability in trophectoderm commitment may be connected to implantation timing. For example, uterine implantation occurs after gastrulation in bovine embryos; approximately two weeks post-blastocyst formation (Berg et al., 2010). Mouse embryos implant and undergo extensive trophectoderm proliferation and differentiation, forming giant cells, ectoplacental cone, and extraembryonic ectoderm within 24 hours of blastocyst formation.

I show that imprinted XCI is established throughout the embryo prior to trophectoderm lineage commitment. Given that the majority of cells in the blastocyst are specified to trophectoderm, I propose that imprinted XCI is globally established in the early

blastocyst in order to ensure that the Xp is silenced before the trophectoderm is committed. It is likely more favorable for the embryo to initiate imprinted XCI in all cells, rather than risk the absence of X-chromosome dosage compensation in trophectoderm. This hypothesis is supported by phenotypic analysis of female embryos that have inherited mutations rendering imprinted XCI unstable in the trophectoderm; these embryos exhibit substantial loss of the trophectoderm-derived tissues, such as the extraembryonic ectoderm and the ectoplacental cone (Wang et al., 2001). Thus, the absence of dosage compensation in the committed multipotent trophectoderm is incompatible with development. Given that bovine embryos exhibit delayed trophectoderm commitment, it would be very interesting to compare the kinetics of Xp silencing between bovine and mouse.

D) Materials and Methods

Embryo collection and Immunosurgery

Embryos were collected from natural mating of *Mus. domesticus* CD1 females to CD1 males carrying the X-GFP (D4.EGFP) transgene (Hadjantonakis et al., 1998). CD1 animals were obtained from Charles River Laboratory. Female blastocysts were distinguished from males by *GFP* expression. Mice were exposed to light daily between 6:00AM and 6:00PM. The morning of the day the plug was detected was considered E0.5. Early blastocysts were collected between E2.75 and E3.0 (approximately 66-72 hours post-copulation). Because embryos collected at the same time varied in developmental stage, blastocysts were also staged according to relative size (a qualitative measure of total cell number) and blastoceol cavity expansion. Early blastocysts can be distinguished by the absence of or a small blastoceol cavity.

Immunosurgery procedures were performed as previously described (Solter and Knowles, 1975). Blastocysts were flushed out of the uterus into room temperature M2 media (Millipore, EmbroMax #MR-015-D). Zona pellucidae were removed by washing blastocysts through Acidic Tyrode's Solution (Sigma, T1788). Embryos were allowed to recover for 5 minutes in room temperature M2 after zona pellucida removal. Subsequent steps were performed in 20 μl drops of media covered with a layer of light mineral oil in a 35mm tissue culture dish. The embryo culture dish was pre-equilibrated at 37°C with 5% CO_2. First, embryos were incubated for 30 minutes at 37°C with 5% CO_2 in whole anti-moue serum produced in rabbit (Sigma, M5774) diluted 1:10 with M2 media. Second, embryos were washed five times with M2 media. For each wash, embryos were allowed to sit in 20ul of M2 media for 5 minutes. Finally, embryos were incubated for 30 minutes at 37°C with 5% CO_2 in guinea pig complement (isolated previously by Terry Magnuson) diluted 1:10 in M2 media. After incubating in guinea pig complement, trophectoderm cells are lysed. Trophectoderm cells were removed by manually pipetting up and down using a finally drawn mouth pipette.

RNA FISH

FISH probes were generated from BAC and FOSMID clones ordered through bacpac.chor.org. 100 ng of probe DNA was labeled using Bioprime Labeling Kit (Invitrogen) with FITC-dUTP (Roche), Cy3-dCTP (GE Healthcare), or Cy5-dCTP (GE Healthcare). The BACs and FOSMIDs are as follows: G135P65743A11 (Ube1x); G135P67639H10 (Mecp2); G135P63425C4 (Xist/Tsix); G135P605237C7 (Rnf12); G135P62497G3 and G135P64951A11 (Atp7a); RP24_274B9 (Abcb7); G135P60362749 (Smcx); and G135P60684137 (Nanog). BACs and FOSMIDs were chosen so that they did

not over lap multiple X-linked genes. All RNA FISH probes used to detect X-linked genes were tested in trophoblast (TS) cell lines to determine detection of X-linked sequences with expected expression patterns. The *Nanog* probe was tested in ES cell lines. 300 μg of yeast tRNA (Invitrogen), 15 μg of mouse Cot-1 DNA (Invitrogen), 100 μl of sheared, boiled Salmon Sperm DNA (Invitrogen), and 10 μl of 3M NaAcetate were precipitated with 100 μl of labeled FISH probe in 100% ethanol by centrifuging for 30 minutes at maximum speed. The precipitated probe was washed once in 70% ethanol, once in 100% ethanol, and then air-dried to remove all traces of ethanol. The dried pellet was resuspended in 50 μl of 100% Formamide, denatured for 10 minutes at 80°C, and then cooled on ice. 50 μl of hybridization buffer (1 part RNAse free water, 1 part RNAase free 20XSSC, 1 part 10mg/ml RNAse free Bovine Serum Albumin, and 2 parts Dextran Sulfate) was then added. The probe mixture was vortex and then pre-annealed at 37°C for 1 hour. Finally, the probe was stored for repeated use at -20°C.

ICMs were prepared for RNA FISH by incubating in 0.05% trypsin just until the individual nuclei in the ICM cluster were visibly distinguishable (no fixed time was determined, I simply watched the ICM in trypsin). Typically, incubation time was under 30 seconds. It is important not to dissociate the ICM into individual nuclei because this will make pipetting impossible; keep the ICM as a cluster of cells. ICMs were then washed through M2 plus 10% fetal calf serum in order to neutralize the trypsin. ICMs were permeabilized for 15 seconds in cytoskeletal buffer (CSK), 1 minute in CSK plus 0.05% triton-X, and 15 seconds in CSK. The recipe for CSK is: 100mM NaCl; 300mM Sucrose; 3mM $MgCl_2$; and 10mM PIPES pH6.8. Bring CSK up to final volume with sterile RNAse free water and store the CSK at 4°C. An aliquot of CSK was taken made fresh prior to each

experiment, RNAsin (Invitrogen, 10441020) was added, and all incubations were performed on a cold block. Finally, ICMs were mounted onto coverslips that were previously coated with 1x Denhardt's Solution (Sigma, 30915) in CSK plus 1% Paraformaldehye (paraformaldehyde was diluted in 1xPBS plus 6mg/ml BSA). After the ICMs have laid down on coverslips, the CSK plus 1% paraformaldehye is gently pipetted off of the ICMs. Because of the trypsin treatment, this sucking action should cause the ICM clusters to flatten out on the coverslips. Coverslips were then air dried for 10 minutes and stored in 70% ethanol at -20°C until ready to use for RNA FISH.

ICMs were dehydrated through an ethanol series of 80%, 90%, and 100% ethanol follow by then air-drying to remove the ethanol. For each coverslip, 10 μl of precipitated RNA FISH probe was hybridized overnight at 37°C. Next day, washes were performed at 42°C: 3 washes with 50% Formamide/2XSSC, 3 washes with 2XSSC, and 2 washes with 1XSSC. Coverslips were mounted onto glass slides with Vectashield plus DAPI mounting media (Vector Labs, H-1500).

Microscopy

Images for RNA FISH were obtained using a Leica DML fluorescence microscope with a Q-imaging Retiga 200R camera and Q-capture software. Images were processed using SPOT RT Software (Diagnostic Instruments). Images for immunostaining were obtained using the Zeiss 710 confocal microscope and processed using the Zeiss software.

Immunostaining

Immunostaining was performed in Terasaki culture dishes. Blastocysts (with zona pellucida removed) were fixed in 3% paraformaldehye diluted in 1xPBS plus 6mg/ml BSA

for 10 minutes at 25°C. After washing five times in 1xPBS plus BSA, blastocysts were permeabilized for 15 minutes in 0.5% tritonX-100 diluted in 1xPBS plus BSA then washed again in 1x PBS BSA. Blocking was performed in 10% heat inactivated goat serum for 1 hour at 25°C. Primary antibodies were Nanog (Chemicon, 1:1000) and Cdx2 (Biogenex, 1:200); dilutions were performed in blocking solution. Primary antibody incubations were performed overnight at 4°C, followed by washing in 1x PBS plus BSA, and incubating in secondary antibody for 45 minutes at 25°C. Secondary antibodies coupled to AlexaFlour 594 (Invitrogen A-11037) and AlexaFlour 488 (Invitrogen A-11039) were diluted to 1:500 in 10% goat serum. The embryos were washed in 1x PBS plus 6mg/ml BSA. In order to avoid smashing the blastocyst during mounting, blastocysts were mounted into 0.12 mm deep Secure-Seal spacer wells (Invitrogen Cat. # S24737) that were fixed onto microscope slides. Mounting media was a dilution of 1:1 Vectashield (Vector Labs) with DAPI in 1x PBS (no BSA). Because the mounting media is not a hard set, the slides were stored flat so that the embryos did not move after mounting. This mounting media was used alternative to other medias because the blastocysts did not collapse in the media. Slides were imaged using an upright confocal microscope; this was important because the blastocysts were mounting in the spacer wells. If imaging was performed on an inverted microscope, the blastocysts were prone to move during the imaging making it impossible to obtain Z-stacks.

Chapter 3: Reactivation of Imprinted XCI in the ICM

In Chapter 2, I showed that naïve epiblast cells in the ICM undergo an inactivation-reactivation cycle to prepare for random XCI in the mature epiblast. Detailed analysis of reactivation in the ICM has not yet been performed; I analyzed both the kinetics of Xp-linked gene reactivation and loss of Xi epigenetic modifications to gain insight into mechanisms of XCI.

Given that (1) Xi gene silencing is thought to be a consequence of *Xist* coating and (2) the Xi is enriched for epigenetic marks that are hallmarks of transcriptionally inactive chromatin, a prerequisite of X-linked gene reactivation is hypothesized to be the sequential loss of *Xist* coating, epigenetic modifying proteins, and chromatin modifications. *Xist* coating and PRC2/H3K27me3 enrichment domains are lost from the Xp in the mature ICM of late (fully expanded) blastocysts (~128 cell stage embryo) suggesting that reactivation is initiated at this time (Mak et al., 2004; Okamoto et al., 2004).

A) Reactivation of the Xp occurs in the presence of Xi epigenetic modifications

To investigate the kinetics of Xp reactivation, I first isolated ICMs from mid-stage female blastocysts (~ 32 to 64 cell stage embryo), which is a developmental time point reported to be prior to loss of Xi epigenetic modifications from the Xp. I performed dual immunofluorescence to detect NANOG, which marks epiblast cells in the ICM, and the PRC2 subunit EED. On average 90% of NANOG positive nuclei contained an EED Xp

domain (Mak et al., 2004; Okamoto et al., 2004; Silva et al., 2009) (Figure 6A and B).

Xist coating and EED/PRC2 accumulation on the Xi are surrogate markers of X-linked gene silencing so I investigated the transcriptional status of X-linked genes directly using RNA FISH and allele-specific RT-PCR. Assaying the same five X-linked genes that previously showed predominantly monoallelic expression in early ICMs, I detected biallelic expression in 35-50% of cells from mid-stage ICMs (Figure 6C), depending on the X-linked gene analyzed. Importantly, in all cases of biallelism one of the two X-linked gene signals co-localized with Xp-*Xist* and H3K27me3 accumulation (Figure 6D). For all five X-linked genes analyzed, I observed a statistically significant increase in the average number of biallelic nuclei and a corresponding decrease in monoallelic nuclei ($p<0.01$; Table 1).

I presented in Chapter 2 that for each X-linked gene analyzed, an active paternal allele is present in a low percentage of total ICM and trophectoderm nuclei of early-stage blastocysts. It may be reasonable to assume that Xp expression in the mid-stage ICM is a consequence of escape from Xp silencing in a subset of early-stage ICM nuclei. Importantly, eleven of fifty-three early-stage ICMs exhibited 100% monoallelic nuclei. In contrast, I never analyzed a mid-stage ICM that were100% monoallelic. Cell divisions in the ICM have been reported to occur approximately every 11.5 hours (Bischoff et al., 2008); consequently, cell number can do no more than double between the early to mid-stage of ICM development. For the increasing biallelism to occur due to escape from imprinted XCI, I

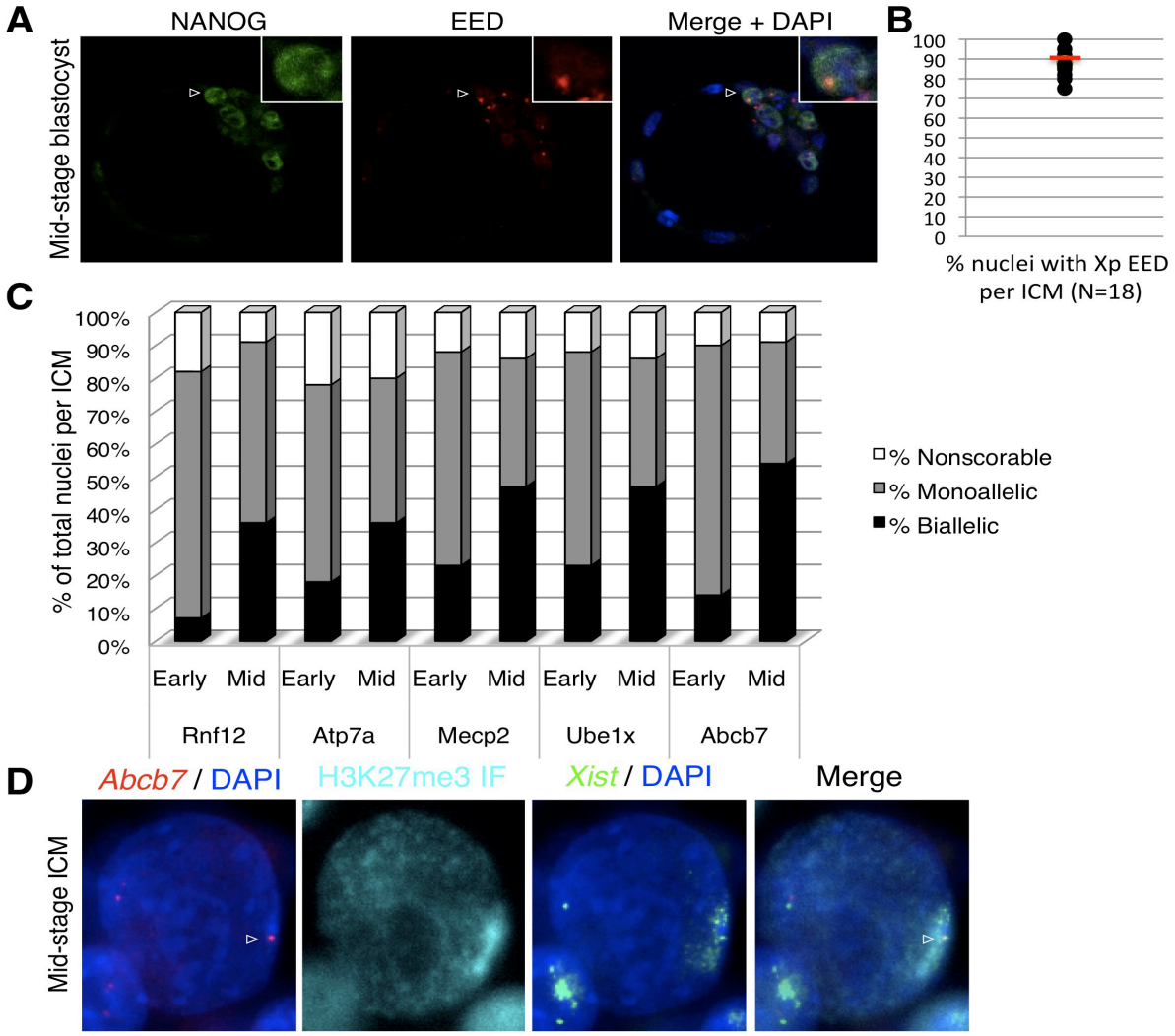

Figure 6 Mid-stage ICMs exhibit increasing Xp expression.

(A) Mid-stage blastocyst immunostained for NANOG (green, left panel) and EED (red, middle panel). The cropped nucleus (marked by an arrow) illustrates a NANOG positive nucleus with Xp EED domain. **(B)** The distribution of NANOG positive ICM nuclei exhibiting an Xp EED enrichment domain is graphed. A red bar represents the average. N is the number of mid-stage blastocysts analyzed. **(C)** Distributions of biallelic (black), monoallelic (grey), and nonscorable (white) nuclei presented as an average percentage of nuclei per ICM. In mid-stage ICMs there is a statistically significant ($p<0.01$) increase in biallelism. **(D)** A representative nucleus illustrates biallelic *Abcb7* (red punctate signal) expression. H3K27me3 accumulates on the Xp above genomic levels (cyan domain). The H3K27me3 enrichment domain colocalizes with Xp-*Xist* coating (green cloud). The merge image (fourth panel) indicates that one of the two *Abcb7* RNA FISH signals (marked by an arrowhead) colocalizes with both the Xp *Xist* and H3K27me3 domains. Nuclei are stained with DAPI.

Table 1 The percentage of monoallelic, biallelic, and nonscorable nuclei measured by RNA FISH in early and mid-stage ICMs

Gene	Stage	n [1]	Mean % Biallelism (per embryo)	% St. Dev.	Mean % Monoallelism (per embryo)	% St. Dev.	Mean % Nonscorable (Nuclei per embryo)	% St. Dev.	P-value [2]	P-value [3]
Ube1x	Early	14	23	13	65	19	12	20		
	Mid	7	47	10	39	11	11	14	0.97	8.735X10-6
Mecp2	Early	15	18	15	60	14	22	18		
	Mid	20	44	13	37	18	18	20	0.94	1.563X10-10
Abcb7	Early	9	14	12	75	8	10	7		
	Mid	7	54	12	37	11	9	11	0.66	9.587X10-10
Rnf12	Early	8	7	8	75	23	16	22		
	Mid	20	36	23	55	27	9	15	0.44	1.825X10-7
Atp7a	Early	7	8	5	76	13	16	16		
	Mid	10	36	13	44	15	20	16	0.78	2.235X10-7

[1] n equals the number of female ICMs.

[2] P values were calculated using a binomial exact test. The null hypothesis is that for each X-linked gene analyzed, the number of nonscorable nuclei is the same between early and mistage ICMs. We reject the null hypothesis when $p<0.01$. In all cases examined, failure to reject the null hypothesis indicates that the number of nonscorable nuclei is not statistically different between early and mid-stage ICMs.

[3] Fisher's Exact test was used to calculate p-values. The null hypothesis is that the average % of biallelic and monoallelic nuclei is the same between early and mid-stage ICMs. We reject the null hypothesis if $p<0.01$ indicating in all cases there is a statistically significant difference between average % of biallelic and monoallelic nuclei between early and mid-stage ICMs.

would have to assume that the small population of biallelic nuclei divided at a rate approximately three times faster than monoallelic nuclei in the early stage ICM. Currently, there is no evidence of any preferential cell divisions occuring in the ICM. Ruling out Xp transcription as a consequence of escape, Xp genic reactivation occurs earlier than previously determined by analysis of inactive-X epigenetic markers. Remarkably, genic reactivation is also evident in the presence of Xp-*Xist* coating and H3K27me3 accumulation on the Xp.

There is some evidence that repressed genes can be poised for expression, producing truncated transcripts prior to transcriptional activation. To confirm our RNA FISH results, I isolated poly-adenylated mRNA transcripts from individual ICMs obtained from crosses between *M. domesticus* (CD1) and *M. molossinus* (JF1) strains. Utilizing single nucleotide polymorphisms (SNPs) between the two mouse strains, I determined the allelic distribution of X-linked gene transcripts by quantitative RT-PCR. I first measured expression of *Xist* RNA. In early F1 ICMs, *Xist* transcription was detectable exclusively from the Xp (Figure 7A). At mid-stage, *Xist* transcription was maintained on the Xp (Figure 7A) consistent with Xp-*Xist* coating, which was evident by RNA FISH (Figure 6E). I next quantified the expression of maternal and paternal alleles for four X-linked genes (*Ube1x, Rnf12, Ddx3x*, *Pdha1*), which were previously determined to exhibited imprinted Xp silencing in extraembryonic tissues (Kalantry et al., 2009). All four X-linked genes exhibited biased Xm expression in early ICMs (Figure 7A). For *Ube1x* and *Rnf12* very little Xp expression could be detected in early ICMs. Paternal silencing of *Pdha1* and *Ddx3x* was less complete but still favored expression from the Xm. These data agree with our RNA FISH results and verify that imprinted XCI is present in early stage ICMs. In contrast, when individual mid-stage

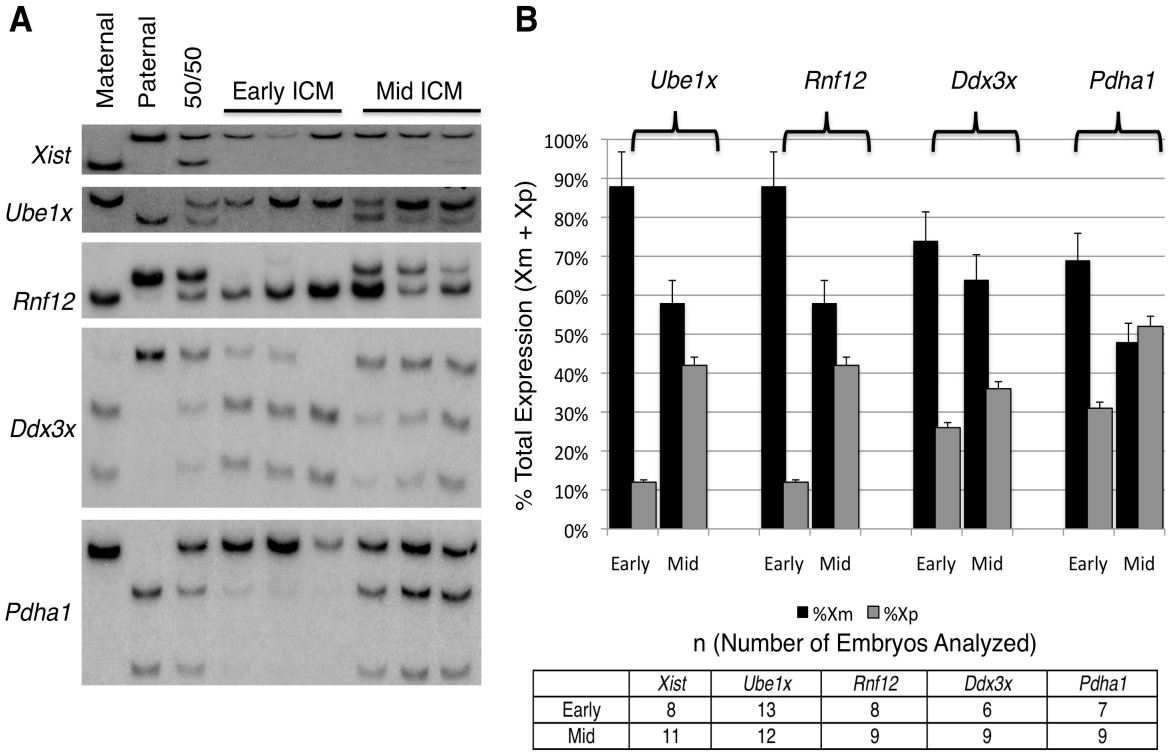

n (Number of Embryos Analyzed)

	Xist	*Ube1x*	*Rnf12*	*Ddx3x*	*Pdha1*
Early	8	13	8	6	7
Mid	11	12	9	9	9

Figure 7 X-linked gene expression assayed by allele-specific RT-PCR.

Mating JF1 females to CD1 males generated F1 hybrid embryos. Xm and Xp transcripts were distinguished utilizing single nucleotide polymorphisms between the two strains. **(A)** Allele-specific expression was analyzed for *Xist*, *Ube1x, Rnf12, Pdha1*, and *Ddx3x*. Lane 1, Xm allele; Lane 2, Xp allele; Lane 3 equal amounts of Xm and Xp allele; Lanes 4-6 representative early F1 hybrid ICM samples; Lane 7-9 representative mid-stage F1 hybrid ICM samples. Analysis of *Xist* expression illustrates that in both early and mid-stage ICMs, *Xist* is expressed from the Xp. In early ICMs, X-linked gene expression for *Ube1x*, *Rnf12*, *Pdha1*, and *Ddx3x* is largely from the Xm allele. In mid-stage ICMs there is increasing Xp expression of Xp-linked genes. **(B)** Average Xm and Xp contributions were calculated as a percentage of total expression (Xm+Xp). There is a statistically significant increase in average Xp expression in mid-stage ICMs for each X-linked gene analyzed ($p<0.01$). The number of ICMs examined is presented in the table.

Table 2 Mean Percentage of Xp expression as measured by Allele-specific RT-PCR

Gene	Stage	n (number of ICMs)	Mean % Xp %Xp= ((Xp)/(Xp+Xm)%)	Standard Deviation	P-value[1]
Ube1x	Early	13	12%	0.17	0.000036
	Mid	12	41%	0.05	
Rnf12	Early	8	5%	0.10	0.00013
	Mid	9	37%	0.15	
Ddx3x	Early	3	26%	0.02	0.014
	Mid	9	36%	0.08	
Pdha1	Early	7	31%	0.16	0.0096
	Mid	9	52%	0.07	

[1] P values were calculated using two-tailed t-tests where the null hypothesis was that for each X-linked gene analyzed the % Xp expression was the same between early and mid ICMs. We reject the null hypothesis when $p>0.05$.

ICMs were analyzed; robust expression from the paternal allele was detected (Figure 7A). *Ube1x*, *Rnf12, Pdha1, and Ddx3x* all exhibited a statistically significant increase in paternal X-linked gene expression in mid-stage as compared to early ICMs ($p<0.05$; Figure 7B, Table 2). These data illustrate the detection of not only nascent transcripts but also spliced polyadenylated transcripts confirming an increase in Xp-linked gene expression in mid-stage ICMs.

B) Reactivation of Xp-linked genes occurs exclusively in the epiblast lineage

We next investigated if biallelic gene expression evident in mid-stage ICMs corresponded to the epiblast cell fate. Lineage commitment in the maturing ICM is illustrated by the progressive upregulation and mutually exclusive expression of lineage markers *Nanog* (epiblast) and *Gata6* (primitive endoderm), which is resolved from uniform expression of these markers in the early ICM (Chazaud et al., 2006). We analyzed NANOG and GATA6 protein in mid-stage blastocysts (Fig. 9A). At mid-stage NANOG and GATA6 are not mutually exclusively in the ICM (Plusa et al., 2008). However, we reasoned that changes in protein products might lag behind changes in gene expression; consequently, analysis of primary transcripts by RNA FISH might confer a more accurate expression pattern of *Nanog* and *Gata6* to be utilized for lineage markers. We found that *Nanog* and *Gata6* nascent transcripts in mid-stage ICMs are largely detected as mutually exclusive cell populations (Fig. 9B). On average approximately 47% of cells per ICM exhibited exclusive *Nanog* expression. In contrast, approximately 32% of cells exhibited exclusive *Gata6* expression. On average 21% of cells per ICM co-expressed both lineage markers (Fig. 9B). The degree of mutually exclusive lineage marker expression appears to depend upon the

maturity of the blastocyst with more developed blastocysts exhibiting fewer cells with coexpression. These data correspond to patterns of *Nanog* and *Gata6* expressions, predicted by protein localization at later stages of ICM development, and validate the use of RNA FISH to measure *Nanog* expression in mid-stage ICMs (Plusa et al., 2008).

Restriction of *Nanog* expression to epiblast progenitors appeared more complete in further developed mid-stage blastocysts. Therefore, in the following experiments, I limited our assays to isolated ICMs from blastocysts of approximately 58-64 cells. In these ICMs, I assayed *Nanog* expression in cells that exhibited biallelic expression of X-linked genes *Atp7a* and *Mecp2*. I found that most cells expressing *Atp7a* and *Mecp2* from both X-chromosomes also expressed *Nanog* (Figure 8D). The reverse was true for *Gata6* expression, which when assayed in independent experiments, was rarely detected in cells exhibiting biallelic X-linked gene expression (Fig. 9D). Utilizing *Nanog* as an epiblast specific marker, I located the cells exhibiting biallelic X-linked gene expression to the epiblast progenitor population. Biallelic gene expression is therefore biased to the epiblast cell fate and not simply a function of incomplete Xp silencing during preimplantation development. I conclude that Xp expression in mid-stage ICMs is a result of reversing imprinted XCI.

C) Chromosome-wide transcription occurs in the presence of *Xist* Coating

Together, our RNA FISH and allele-specific RT-PCR results show reactivation of seven Xp-linked genes occurs in the presence of Xp-*Xist* coating. In order to determine the broader transcriptional status of the Xp, I next hybridized with a Cot-1 DNA probe and *Xist* probe in our RNA FISH experiments. Under RNA FISH conditions, Cot-1 DNA hybridizes to transcribed repetitive sequences of the genome, both inter- and intragenic (Hall et al., 2002). In combination with a *Xist* probe, Cot-1 RNA FISH has been previously utilized for

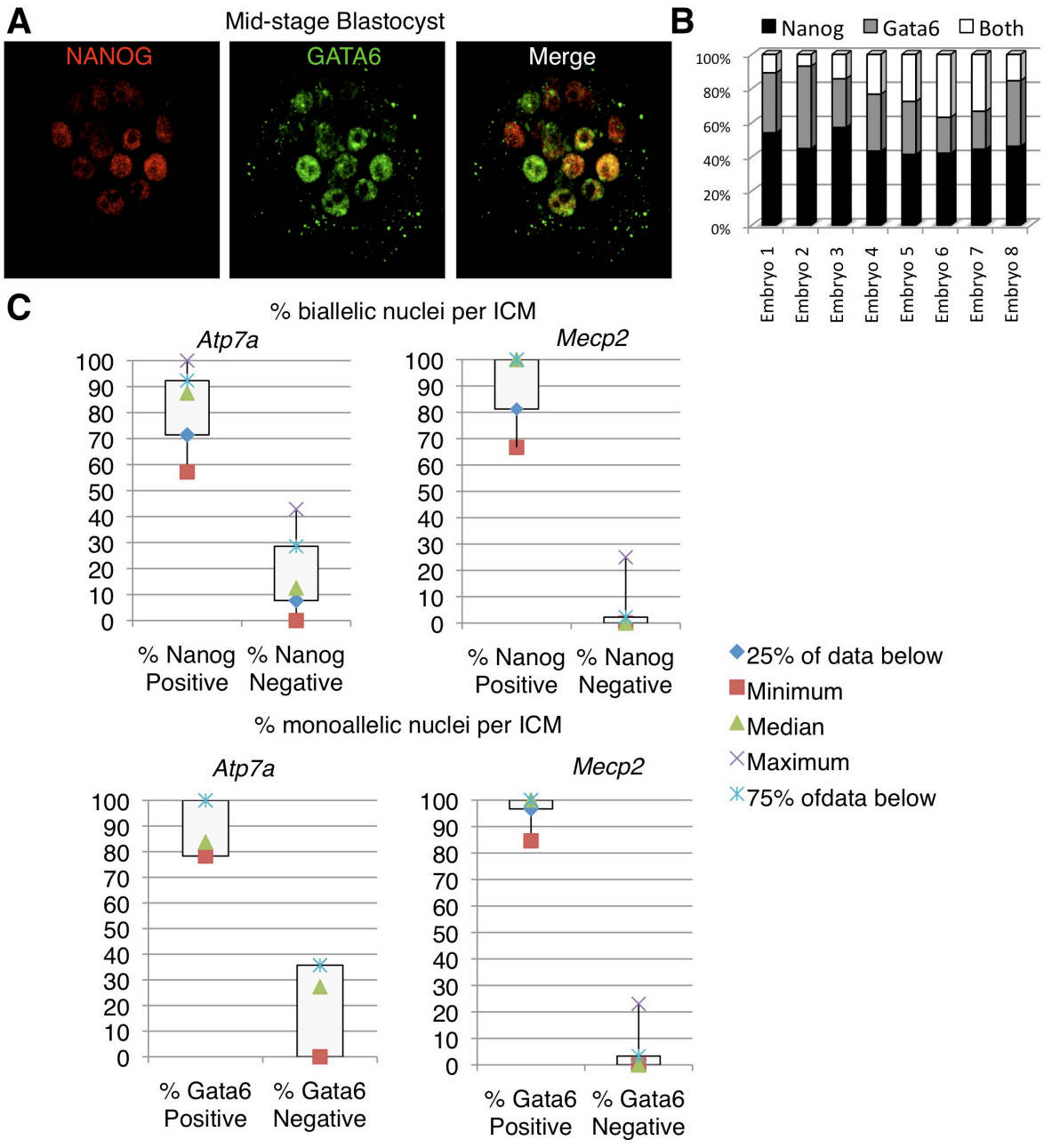

Figure 8 *Nanog* transcripts are associated with biallelic X-linked gene expression.

(A) Colocalization of NANOG and GATA6 (merge) can be detected in some ICM cells at mid-stage. **(B)** The distribution of *Nanog* (black) and *Gata6* (grey) transcripts measured by RNA FISH is graphed as % of total cells per ICM. The majority of cells exhibit mutually exclusive transcription of *Nanog* (black) and *Gata6* (grey). **(C)** The % nuclei per mid-stage ICM (y-axis) that scored positive or negative for *Nanog* (top box plots) and *Gata6* (bottom box plots) transcripts (x-axis) are graphed in side-by-side boxplots for X-linked genes *Atp7a* (left) and *Mecp2* (right). Nonoverlapping boxplots imply that biallelic cells are skewed toward Nanog expression; monoallelic cells are skewed toward *Gata6* expression.

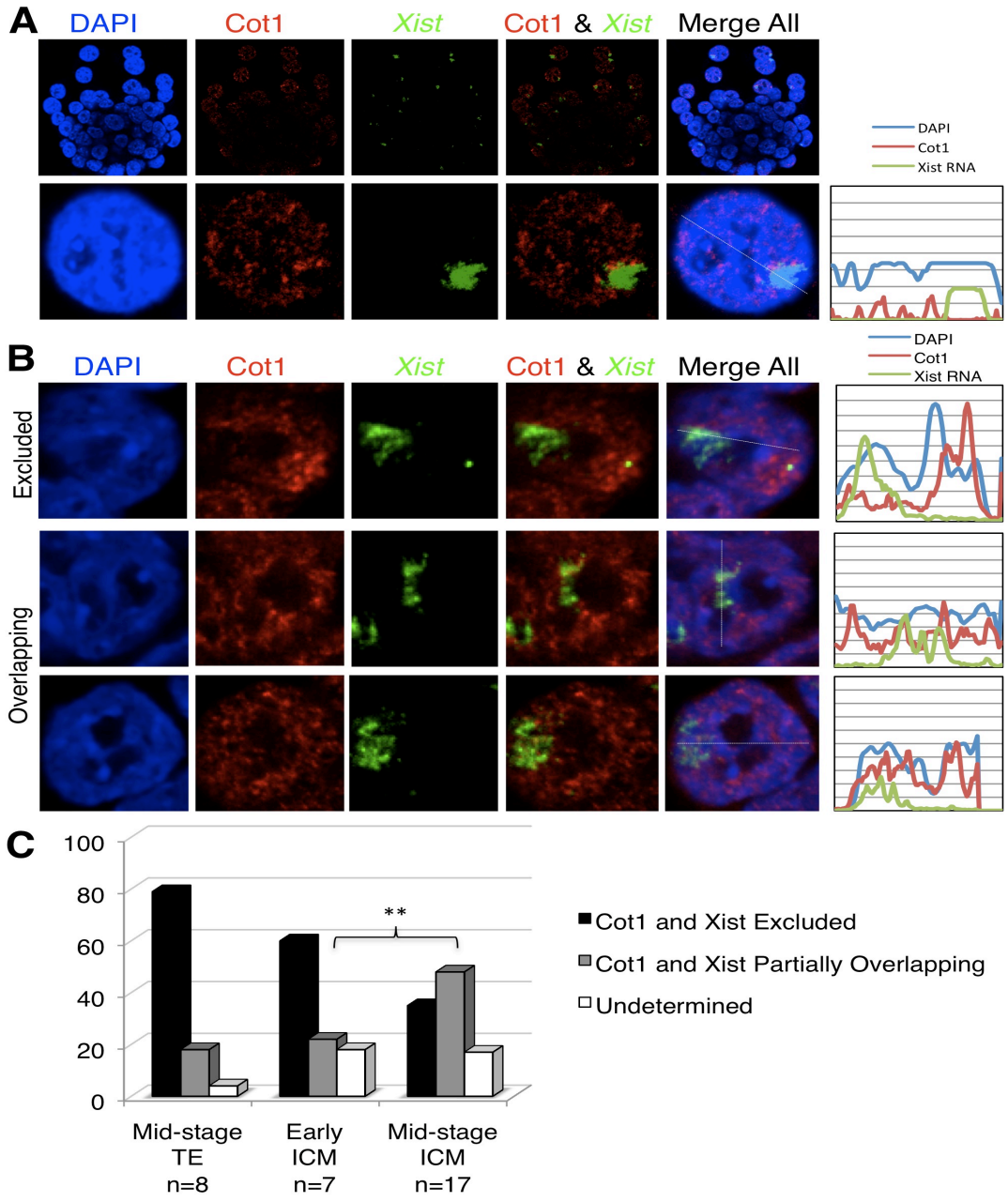

Figure 9 Mid-stage ICMs exhibit transcription within the Xp-*Xist* domain.

Cot-1 DNA (red) and *Xist* (green) probes were used in RNA FISH experiments to determine general Xp transcriptional status. (A) In the trophectoderm, the Cot-1 probe does not hybridize to the *Xist* coated region of the Xp, forming what is referred to as the Cot-1 hole. Line scans indicate the relative intensities of DAPI, Cot-1, and *Xist* signals. (B) Representative mid-stage ICM nuclei indicate mutually excluded or overlapping patterns. (C) The average distribution of nuclei with mutually excluded or overlapping Cot-1 and *Xist* RNA FISH signals are graphed as a percentage of total nuclei per mid-stage trophectoderm (TE), early ICM, and mid-stage ICM. The bracket represents a statistically significant increase in the percentage of cells exhibiting

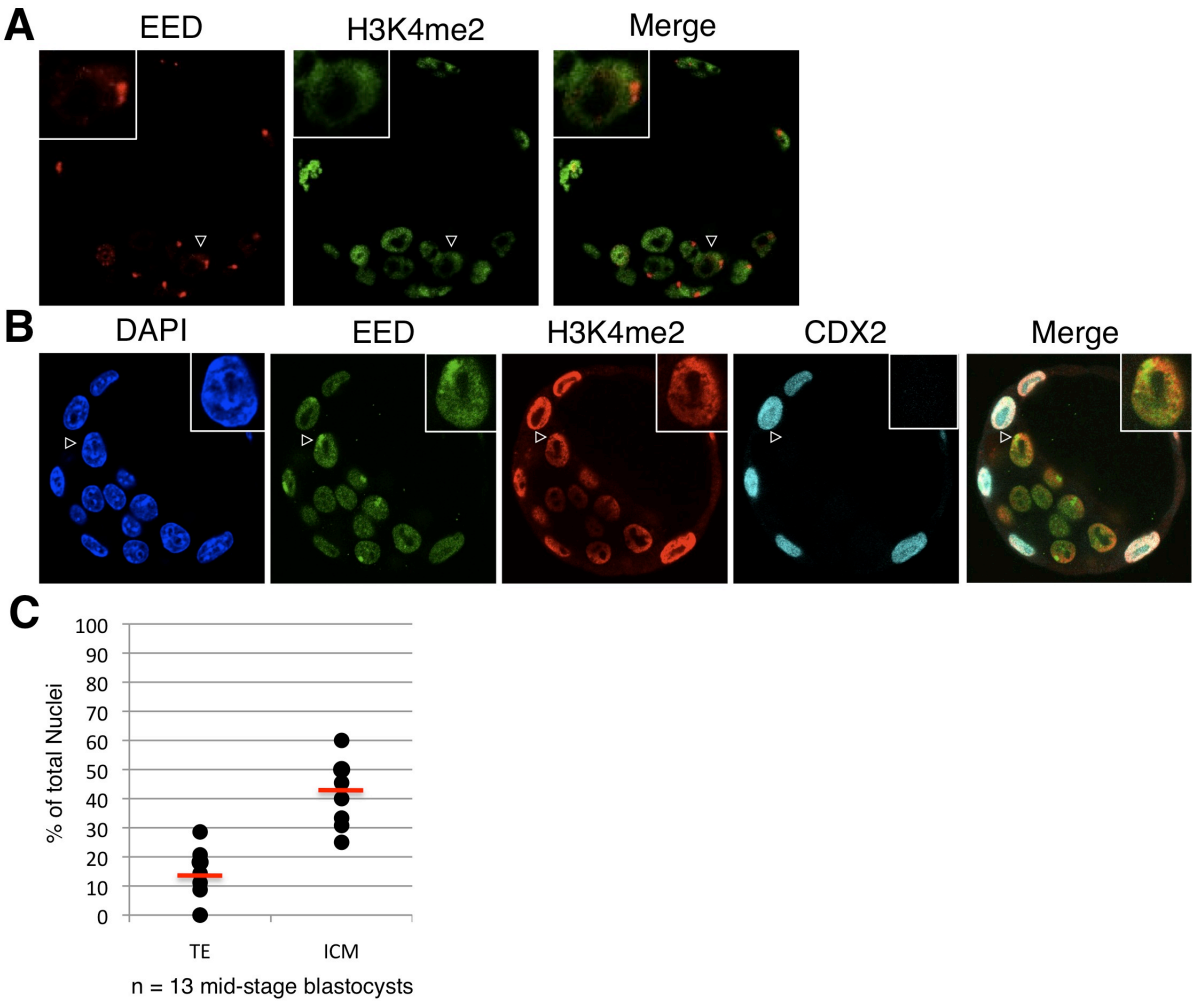

Figure 10 Epigenetic marks associated with transcription overlap the Xp EED domain.

(A) A confocal section of a mid-stage blastocyst immunostained for EED (red, first panel) and H3K4me2 (green, second panel). EED marks the Xp as an enrichment domain. In the cropped image, an ICM nucleus (arrowhead) exhibits H3K4me2 staining, a mark of transcription, within the Xp EED domain (merge, third panel). (B) In order to determine the relative number of ICM nuclei, as compared to CDX2 positive trophectoderm nuclei, that exhibited Xp H3K4me2 staining, blastocysts were immunostained for EED (green, second panel), H3K4me2 (red, third panel), and CDX2 (cyan, fourth panel). In the cropped image, a CDX2 negative nucleus (arrowhead) exhibits H3K4me2 signal overlapping the Xp EED domain (merge, fifth panel). DAPI stains all nuclei. **(C)** The graph represents the distribution of Xp EED domains that exhibit H3K4me2 signal. Distributions are graphed as a percentage of total trophectoderm or total ICM nuclei per embryo. A red line represents the average. N = the number of embryos analyzed.

visualization of general transcription within the *Xist* RNA domain. It has previously been shown that the X-chromosome is devoid of Cot-1 hybridization when gene silencing is established (Chaumeil et al., 2006; Namekawa et al.). Consistent with predominant Xp-silencing, I detected mutually exclusive *Xist* and Cot-1 RNA FISH signals in the majority (~82%) of trophectoderm nuclei of mid-stage blastocysts (Figure 9a). In contrast, when I performed RNA FISH on mid-stage ICMs, I detected nuclei with overlap of Cot-1 and *Xist* RNA FISH signals (Figure 9b). Cot-1 RNA FISH signal typically overlapped the exterior of the intense *Xist* domain although nuclei were also detected that exhibited an Xp-*Xist* domain completely overlapped by Cot-1 RNA FISH signal. I quantified the number of nuclei per mid-stage ICM that exhibited patterns of mutually exclusive or overlapping RNA FISH signals. On average, 45% of nuclei per mid-stage ICM exhibited overlapping signals of Cot-1 and *Xist*. The ICM as compared to the trophectoderm is therefore enriched for nuclei exhibiting Cot-1 signal overlapping the Xp-*Xist* domain. This pattern of overlap is not simply characteristic of ICM cells, in general, as I detected a significant ($p<0.01$) increase in the number of nuclei with overlap when I compared early to mid-ICMs (Figure 9c). This increase in the number of nuclei exhibiting transcription from within the *Xist* RNA domain is consistent with general Xp reactivation occurring in the presence of *Xist* coating. To our knowledge, this is also the first observation that transcription can occur within an *Xist* domain, as previously *Xist* coating was thought to cause formation of the Xi silent domain, which has typically been defined by the absence of Cot-1 RNA FISH signal (Chaumeil et al., 2006).

D) H3K4me2 overlaps the Xp EED domain

Once XCI is established, the chromatin of an inactive X-chromosome is characterized by depletion of histone modifications associated with gene expression. This depletion can be detected at the cytological level by exclusion of di-methylation of histone H3 at lysine 4 (H3K4me2) from the Xp EED domain. I performed immunostaining on mid-stage blastocyst to detect H3K4me2 and EED (Figure 10A and B). ICM nuclei were distinguished by the absence of CDX2, a marker of trophectoderm (Figure 10B). In the preimplantation stage embryo, some nuclei in the mid-stage blastocyst exhibited H3K4me2 signal that overlapped the Xp EED domain, suggestive of general Xp transcription. I observed an average 12% of trophectoderm nuclei with this staining pattern. In contrast, an average 43% of CDX2 negative ICM nuclei exhibit H3K4me2 staining that overlaps the Xp EED domain (Figure 10C). The relative preference for this staining pattern in the ICM, relative to trophectoderm nuclei of the same embryo, is consistent with Xp reactivation. It is also interesting that the Xp in both ICM and trophectoderm nuclei exhibited general Xp transcription in the presence of both *Xist* coating (Figure 9C) and PRC2 (Figure 10A and B); these surrogate markers of XCI are likely unable to prevent transcription, irrespective of lineage.

E) Conclusions

Here, I present evidence that reversal of imprinted XCI initiates earlier than previously determined by analysis of Xi epigenetic markers. Reactivation of the Xp, as evident by an increase in Xp-linked gene activity, initiates in the mid-stage ICM coincident with, rather than as a consequence of, epiblast lineage specification. Chromosome-wide transcription is evident in the presence of *Xist* coating, as well as the cytologically detectable PRC2 and H3K27me3 domains. Together, these observations suggest that, particularly at

this early stage of embryonic development, these epigenetic marks classically analyzed at the cytological level to generalize X-chromosome activity do not accurately reflect the expression state of individual X-linked genes. The concept that reactivation of X-linked genes could occur in the presence of the chromatin modification H3K27me3, which is known to stabilize XCI, is especially surprising. I suggest two possible explanations for our observations.

First, it is currently speculated that *Xist* RNA recruits PRC2 to the X-chromosome (Zhao et al., 2010). The mechanism of how this recruitment occurs, and how H3K27me3 is spread to decorate the entirety of X-chromosome chromatin, is poorly understood. It is possible that *Xist* does not coat the entire X-chromosome in a linear fashion. *Xist* transcripts may favor certain DNA sequences defined as booster elements (Gartler and Riggs, 1983). *Xist* transcripts can associate with autosomal DNA sequences, suggesting that *Xist* coating is not dependent on unique X-linked gene sequences. This led to the hypothesis that repetitive sequences may function as booster elements (Lyon, 1998). A possible explanation for ICM reactivation in the presence of *Xist* coating is that, even though *Xist* and PRC2/H3K27me3 are detected cytologically to accumulate on the Xp, the spread of these epigenetic modifications may be incomplete. In both early and mid-stage ICMs, *Xist* coating and PRC2/H3K27me3 may not have reached all genic loci. In the absence of epigenetic modifications at individual loci, there exists no block to prevent gene specific reactivation occurring prior to the chromosome-wide removal of epigenetic modifications. Due to the small number of cells and heterogeneity in the developing ICM, I are limited to cytological detection of these epigenetic modifications, which is at low resolution as compared to the level of DNA sequence. In the future with improvements in technology, high-resolution

analysis of H3K27me3 by chromatin immunoprecipitation will determine how this modification spreads to genic loci during preimplantation development.

The above explanation suggests that genic reactivation in the ICM can be explained by piecemeal spreading of Xi epigenetic modifications across the Xp. Recent data have shown that *Xist* transcripts first concentrate near the *Xist* locus and then coating spreads to the rest of the chromosome (Sarma et al., 2010). This is consistent with the long held opinion that gene silencing occurs first at X-linked genes located nearest the *Xist* locus, extends linearly to distant regions of the X-chromosome (Huynh and Lee, 2003). Although our study analyzes a subset of X-linked genes, the proximity to *Xist* had no consequence in the propensity to reactivate. The seven X-linked genes analyzed were chosen at random and are located along the length of the X-chromosome; yet all genes exhibited reactivation in the presence of *Xist*/PRC2 accumulation. The absence of repetitive element silencing and the presence of H3K4me2 immunostaining on the Xp also indicated chromosome-wide reactivation. I argue it is unlikely the reactivation I have observed is due to a propensity of a subset of X-linked genes to reactivate.

I therefore favor a second possible explanation for reactivation in the presence of PRC2/H3K27me3 enrichment. While H3K27me3 is a chromatin modification generally associated with gene repression, the exact mechanism for how H3K27me3 inhibits transcription is unknown. I have shown microscopically that the Xp in ICMs is enriched for both H3K4me2 and H3K27me3. In ES cells, 'bivalent' genes have been defined by the presence of both active and repressive histone modifications, particularly the presence of H3K4me3 and H3K27me3. It was originally reported that these bivalent genes were transcriptionally inert (Boyer et al., 2006; Lee et al., 2006). However, utilizing more

sensitive assays recent results indicate that 'bivalent genes' exhibiting H3K4me3 and H3K27me3 have engaged RNA Polymerase II at the transcription start site. In addition, while these genes exhibit reduced expression levels compared to the genome average, a significant amount of productive RNA Polymerase II elongation was detected (Min et al., 2011). These data indicate that in the presence of epigenetic marks associated with activation, H3K27me3 may not be sufficient to block productive transcription. A minority of X-linked genes has been shown to escape XCI in somatic tissues, usually in a tissue-specific manner (Reinius et al., 2010). Interestingly, CHIP-sequencing and RNA-sequencing in TS cells have been performed by a postdoctoral fellow in our lab, Mauro Calabrese; in Calabrese et al., he shows that a subset of escaping genes are bound by PRC2 and exhibit H3K27me3, again indicating that this histone modification associated with XCI is not sufficient to prevent X-linked gene expression.

F) Materials and Methods

Embryo collection and Immunosurgery

Embryos were collected from natural mating of either *Mus. domesticus* CD1 females (RNA FISH) or *Mus. molossinus* JF1 females (RT-PCR) to CD1 males carrying the X-GFP (D4.EGFP) transgene (Hadjantonakis et al., 1998). Female blastocysts were distinguished from males by *GFP* expression. Mice were exposed to light daily between 6:00AM and 6:00PM. The morning of the day the plug was detected was considered E0.5. Early blastocysts were collected between E2.75 and E3.0 (approximately 66-72 hours post-copulation). Mid-stage blastocysts were collected between E3.5 and E3.75 (approximately 84-90 hours post-copulation). Mid-stage blastocysts were distinguished from early-stage

blastocysts because the blastoceol cavity was expanded by the mid-stage. Immunosurgery procedures were performed as previously described in Chapter 2.

Immunostaining

Protocols for immunostaining were described in Chapter 2. Primary antibodies were Nanog (Chemicon, 1:1000), Cdx2 (Biogenex, 1:200), Gata6 (R&D Systems 1:1000), H3K27me3 (Upstate, 1:250), H3K4me2 (Upstate, 1:100), and EED (Arie Otte, Slater Institute, Amsterdam, The Netherlands, 1:200).

RNA FISH

RNA FISH probes were previously listed in Chapter 2, except for the Gata6 probe that was RP24_329F11. To detect repetitive sequence expression, Mouse Cot-1 DNA (Invitrogen) was used as a RNA FISH probe. The labeling and precipitation protocol was described in Chapter 2 with one modification that Cot-1 DNA is not added as a blocking agent in the precipitation protocol. *Gata6* FISH probes were tested in ES and extraembryonic endoderm (XEN) cell lines, respectively.

For combined immunostaining of H3K27me3 and RNA FISH, ICMs were permeabilized in CSK for 15 seconds, CSK plus 0.05% tritonX-100 for 30 seconds, CSK for 15 seconds, and then plated onto 1x Denhardt's coated coverslips in CSK plus 1% paraformaldehye. After air-drying the ICMs on the coverslips, ICMs were fixed in 3% paraformaldehye for 10 minutes at room temperature. ICMs were immediately prepared for immunostaining. Immunostaining was performed as described in Chapter 2 with the exceptions that the 0.05% tritonX-100 steps is removed and all steps are performed under RNAse free conditions by adding RNAsin to the 1x PBS 6mg/ml BSA and the 10% goat

serum. After immunostaining, ICMs were fixed in 2% paraformaldehye for 5 minutes at room temperature and then immediately prepared as described in Chapter 2 for RNA FISH.

Statistical Analysis of RNA FISH

RNA FISH nuclei were classified as biallelic, monoallelic, or nonscorable/undetermined. Nuclei were classified as nonscorable/undetermined when no RNA FISH signal could be detected. For each X-linked gene, the total number of the three classes of nuclei was compared between early and mid-stage ICMs. Binomial exact test was used to verify that nonscorable data between stages were equivalent. Fisher's Exact test was used to compare the three categories between early and mid-stage ICMs. P values of $p<0.01$ was considered significant. The procedure was repeated for the Cot-1 and *Xist* RNA FISH experiments except the nuclei were scored as either excluded, overlapping, or nonscorable/undetermined.

Microscopy

Images for RNA FISH were obtained using a Leica DML fluorescence microscope with a Q-imaging Retiga 200R camera and Q-capture software. Images were processed using SPOT RT Software (Diagnostic Instruments). For Cot-1/*Xist* RNA FISH and H3K4me2/H3K27me3 immunostaining experiments, images were obtained on a Zeiss710 confocal microscope. Individual confocal sections were analyzed using Zen software to determine overlap between signals. To determine relative intensity values obtained in the Cot-1 RNA FISH experiments, we generated line traces across nuclei using NIH Image J software and used the plot profile tool to measure the intensity across the line traces.

RT-PCR

Polyadenylated mRNA was prepped using the Dynabeads mRNA DIRECT Micro Kit (Invitrogen, 610.21). Individual ICMs were lysed in 100 ul of lysis/binding buffer following manufacturers protocol. For RT-PCR, SuperScript III One-Step RT-PCR Platinum Taq (Invitrogen, 12574-035) was used to amplify the cDNA. A portion of the final RT-PCR product was used to perform one round of amplification in the presence of a trace amount of ^{32}P-dCTP (Perkin Elmer, BLU513H) to minimize heteroduplexes and to radioactively-label the RT-PCR product. The final PCR product was digested with the appropriate restriction enzyme, run on a 10% acrylamide gel, and exposed to film. All RT-PCR primers were previously described (Kalantry et al., 2009). Band intensities were quantified using Adobe Photoshop CS3 Extended software. Percent paternal expression was calculated as a percentage of total intensity of combined maternal and paternal-specific bands (%Xp= Xp/[Xm+Xp]). In case of multiple maternal- or paternal-specific bands, the band intensities were added to yield a single value. The average %Xp expression was compared between early and mid-stage ICMs for each X-linked gene. P-values were calculated using two-tailed t-tests where the null hypothesis is that the mean %Xp of early and mid-stage samples are the same.

Chapter 4: Extinction of *Xist* coating has no effect on Xp genic reactivation

The data presented in Chapter 3 argue against loss of the *Xist* coat as a prerequisite to initiate Xp reactivation. One possibility that may explain reactivation of the Xp in the presence of *Xist* coating, without invoking *Xist*-independent mechanisms for reactivation, is that reduced transcription of the paternal *Xist* allele may occur simultaneously with chromosome-wide reactivation. If so, then nuclei exhibiting biallelic X-linked gene expression represent nuclei with lower levels of *Xist* coating. Thus, decreasing amounts of *Xist* coating could trigger Xp reactivation, supporting the previous models for reprogramming XCI.

In the ICM, I saw no indication that the amount of *Xist* coating, measured by RNA FISH, was associated with an active Xp; I also detected no obvious differences between the Xp-*Xist* domains in ICM nuclei as compared to trophectoderm nuclei. However, subtle decreases in amount of *Xist* transcripts coating the Xp may be undetectable by RNA FISH. I considered performing quantitative RT-PCR in the context of single cells to measure transcription of Xp-*Xist*, but I ruled out this experiment, as the total abundance of *Xist* transcripts is not a direct measure of the amount of transcripts coating the Xp. It is unclear how *Xist* RNA coats the X-chromosome, but data support the conclusion that *Xist* coating depends, in part on stabilization of *Xist* transcripts in the nucleus (Royce-Tolland et al., 2010). I took an unconventional approach to address the possibility that decreasing amounts of *Xist* coating triggers reactivation. I sought to conditionally deplete *Xist* coating in mid-

stage ICMs. I reasoned that if Xp gene expression were regulated independently of *Xist* RNA then precocious loss of the Xp-*Xist* coating would have no effect on the kinetics of genic reactivation. In contrast, if decreasing levels of *Xist* trigger reactivation, then dramatic loss of *Xist* should trigger Xp reactivation.

A) Increased NANOG dosage results in loss of Xi epigenetic markers of XCI

For these experiments, I took advantage of a genetic mutation in *Grb2*, a key adaptor molecule necessary for MAP kinase signal transduction. Activation of MAPK signaling in both ICMs and ES cells has been shown to negatively regulate *Nanog* expression. Conversely, blocking MAPK signaling in ICMs is believed to release *Nanog* repression, resulting in transformation of primitive endoderm cells to epiblast. Consistent with this hypothesis, *Grb2* $^{-/-}$ embryos exhibit early post-implantation lethality due to a lack of endodermal differentiation (Hamazaki et al., 2006; Pawson and Scott, 1997).

NANOG is highly variable in the mid-stage ICM with strong immunostaining detectable in only a subset of ICM cells. In contrast, *Grb2* $^{-/-}$ blastocysts exhibit strong NANOG immunostaining in the majority of ICM cells (Figure 11A) (Chazaud et al., 2006). *Grb2* $^{-/-}$ blastocysts were phenotypically indistinguishable from littermate controls, and no cell death has been reported in *Grb2* $^{-/-}$ ICMs as compared to littermate controls. It has been reported that NANOG directly represses *Xist* expression in undifferentiated mouse ES cells (Navarro et al., 2008). In support of these results, I observed that female mid-stage E3.5 *Grb2* $^{-/-}$ blastocysts exhibit uniform loss of EED and H3K27me3 Xp enrichment throughout the ICM (Figure 11A, B, and C). I also found a significant reduction in the number of ICM cells with Xp-*Xist* coating in *Grb2* $^{-/-}$ ICMs compared to littermate controls (Figure 12A). I noted that even when Xp-*Xist* coating was detectable in *Grb2* $^{-/-}$ mid-stage ICMs, the density

of the coat was significantly reduced. The depletion of *Xist* coating at mid-stage was in contrast to *Grb2* $^{-/-}$ embryos isolated between the 8- to 16-cell stage, which exhibited normal Xp-*Xist* coating (data not shown). *Xist* coating the Xp in *Grb2* $^{-/-}$ cleavage stage embryos indicates that imprinted XCI initiated normally as would be predicted from the low levels of NANOG reported at the 8-cell stage (Yamanaka et al., 2010). Trophectoderm cells appeared to maintain Xi epigenetic markers in wild type and *Grb2* $^{-/-}$ blastocysts (Figure 11A and B).

B) Ectopic loss of *Xist* coating has no effect on Xp reactivation kinetics

Interestingly, the loss of Xp *Xist* coating in the *Grb2* $^{-/-}$ ICMs did not result in reactivation of Xp genes. For the four genes I analyzed (*Ube1x*, *Rnf12*, *Atp7a,* and *Abcb7*) monoallelic X-linked gene expression was detectable in cells without visible Xp-*Xist* coating (Figure 12B and C). I found similar patterns of monoallelic and biallelic Xp-linked gene expression in female *Grb2* $^{-/-}$ ICMs as compared to female littermate controls, irrespective of the amount of *Xist* coating the Xp (Figure 12B). Despite widespread loss of Xp-*Xist* and Xp-EED accumulation, reactivation in *Grb2* $^{-/-}$ ICMs occurs normally. Analysis of ICM nuclei from late stage blastocysts (~128 cells) also indicates that in the absence of *Xist* coating, Xp silencing can be maintained through cell divisions (Figure 13A and B). These data rule out the possibility that the reactivation detected in the mid-stage ICM is due to subtle decreases in the levels of *Xist* and show that genic silencing in the ICM can be maintained independent of cytologically detectable *Xist* coating and PRC2.

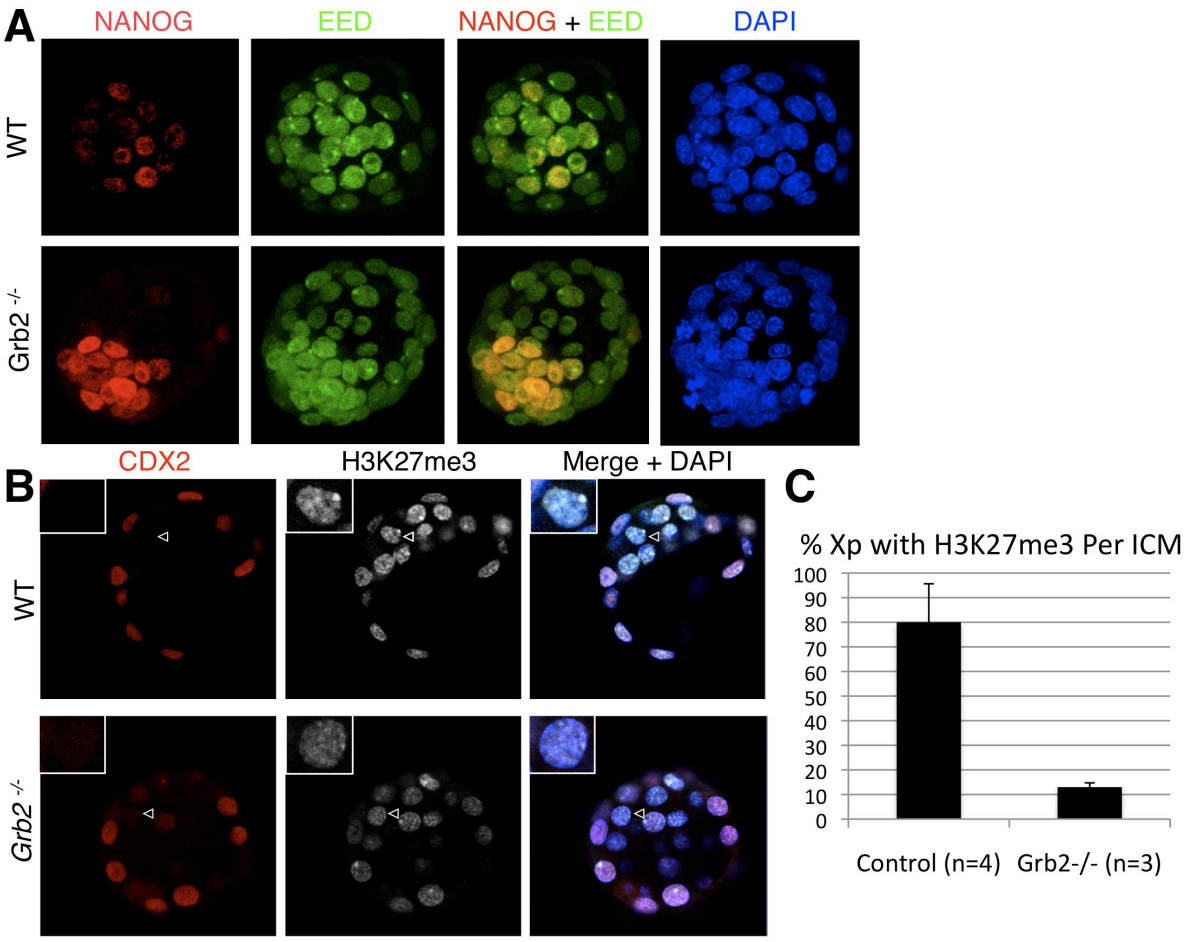

Figure 11 *Grb2* $^{-/-}$ ICM cells exhibit loss of *Xist* transcripts and EED on the Xp.

(A) Mid-stage blastocysts immunostained for NANOG (red, first panels) and EED (green, second panels). In wild type blastocysts (top panels), EED accumulates on the Xp in NANOG positive nuclei as seen by the yellow foci (merge, third panels). However, in all but one NANOG positive nuclei of *Grb2* $^{-/-}$ blastocysts (right panels), Xp EED foci are undetectable (merge, third panels). DAPI stains all nuclei.
(B) Optical sections of mid-stage blastocysts immunostained for CDX2 (red, first panels) and H3K27me3 (white, second panels). DAPI stains all nuclei. The cropped images in the left corners represent ICM nuclei, which are distinguished by the absence of CDX2 staining. Arrowheads also mark the nuclei in the cropped images. In WT ICM nuclei (top row), H3K27me3 accumulated on the Xp. The *Grb2* $^{-/-}$ ICM (bottom row) is characterized by the absence of H3K27me3 Xp enrichment foci.
(C) The graph illustrates the number of H3K27me3 Xp foci detected in ICM nuclei of WT and *Grb2* $^{-/-}$ blastocysts.

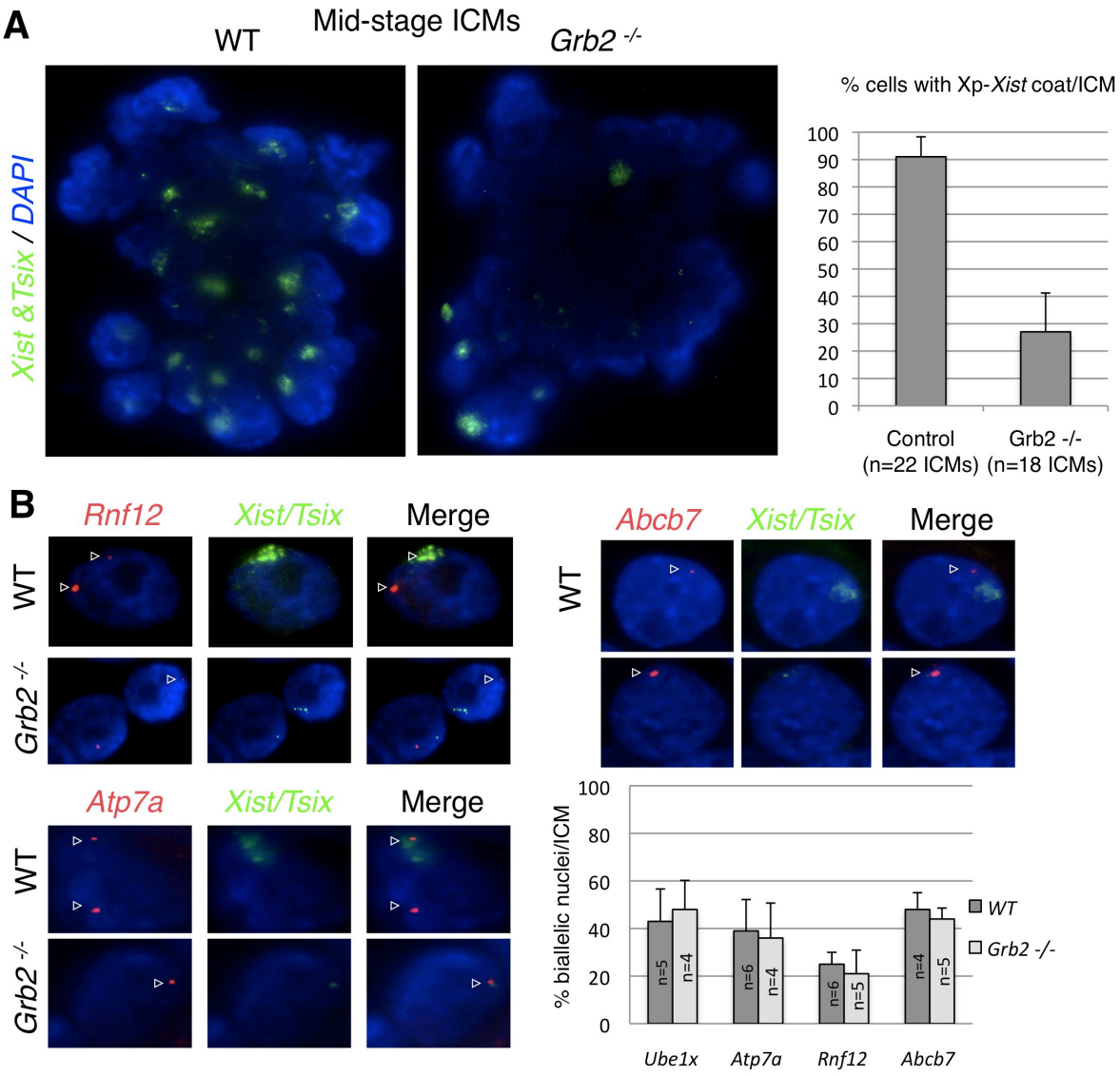

Figure 12 Loss of *Xist* coating does not alter reactivation kinetics.

(A) Wild type (top panels) and *Grb2* $^{-/-}$ (bottom panels) mid-stage ICMs assayed by RNA FISH for transcripts of *Xist/Tsix* (green). The graph indicates the average % of cells per ICM that exhibit *Xist* coating in *Grb2* $^{-/-}$ as compared to wild type littermate controls. **(B)** Nuclei from wild type (upper rows) and *Grb2* $^{-/-}$ (bottom rows) ICMs assayed for transcripts of X-linked genes *Rnf12*, *Atp7a,* and *Abcb7* (red signals marked by arrowheads, left panels) and *Xist/Tsix* (green, middle panels). *Grb2* $^{-/-}$ ICM nuclei (bottom rows) show monoallelic expression in the absence of the Xp-*Xist* domain (merge, right panels). The graph at the right indicates the distribution of biallelic X-linked gene expression in *Grb2* $^{-/-}$ ICMs as compared to wild type. The data are presented as a % of total cells/ICM.

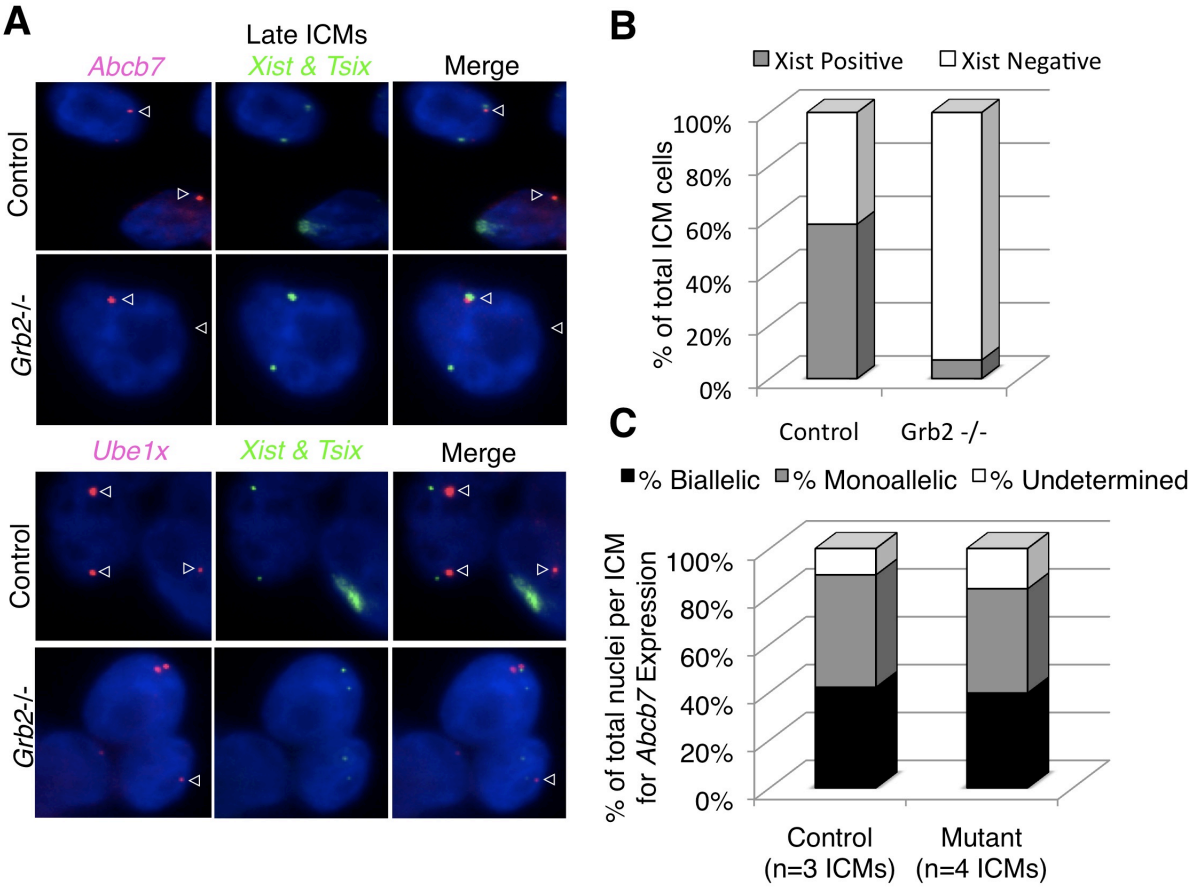

Figure 13 *Grb2*-/- ICM nuclei maintain Xp-linked gene silencing through cell divisions.

(A) RNA FISH was used to analyze X-linked gene expression (red, arrows) and *Xist* (green) in Control and *Grb2*-/- late stage ICMs. Representative images of *Abcb7* expression (top panel) and *Ube1x* expression (bottom panel) are provided. **(B)** The distribution of nuclei in Control and *Grb2*-/- ICMs exhibiting *Xist* coating is indicated in the graph**. (C)** The distribution of monoallelic and biallelic *Abcb7* nuclei is graphed for control and Grb2-/- late stage ICMs. N=number of ICMs analyzed.

C) Maintenance of Imprinted XCI in the blastocysts

Modifications and proteins in addition to PRC2-mediated H3K27me3 have been defined in extraembryonic tissues to maintain XCI (Chong et al., 2007; Garrick et al., 2006; Kohlmaier et al., 2004; Plath et al., 2004). I tested if any of these Xi epigenetic markers are also present on the Xp at the blastocyst stage. Immunostaining for RING1b, H4K20me1, ATRX, and SMCHD1 was first performed on female trophectoderm stem cells (TS cells) (data not shown). TS cells are derived from the trophectoderm of E3.5 blastocysts. Despite localization of ATRX and SMCHD1 in TS cells, only RING1b and H4K20me1 accumulated on the Xp in mid-stage blastocysts (Figure 14A and B). Importantly, while RING1b was detected in some NANOG positive ICM nuclei, RING1b was not found to accumulate on the Xp in all blastocyst nuclei. In fact, a minimal number of nuclei per blastocyst showed RING1b Xp foci (Figure 14B), which is consistent with a previous report (de Napoles et al., 2004). H4K20me1 was weakly detected to accumulate on the Xp at the mid-stage blastocyst, and a significant number of nuclei showed no H4K20me1 foci (Figure 14C). Given these results in WT blastocysts, it is unlikely that the presence of these modifications is responsible for maintenance of Xp silencing, in the absence of *Xist* coating and H3K27me3, which is found in *Grb2* $^{-/-}$ ICMs. Additionally, in undifferentiated EED$^{-/-}$ TS cells, the Xp exhibits not only depletion of H3K27me3 but also depletion of H2A ubiquitination and H4K20 mono-methylation; however, EED$^{-/-}$ TS cells do not exhibit reactivation of the imprinted Xp indicating that these marks are not necessary for silencing (Kalantry et al., 2006).

D) Conclusions

In chapter 4, I have shown that in mid-stage ICMs Xp-genic silencing, at least for a subset of X-linked genes, can be maintained even after inactive-X epigenetic marks, *Xist*

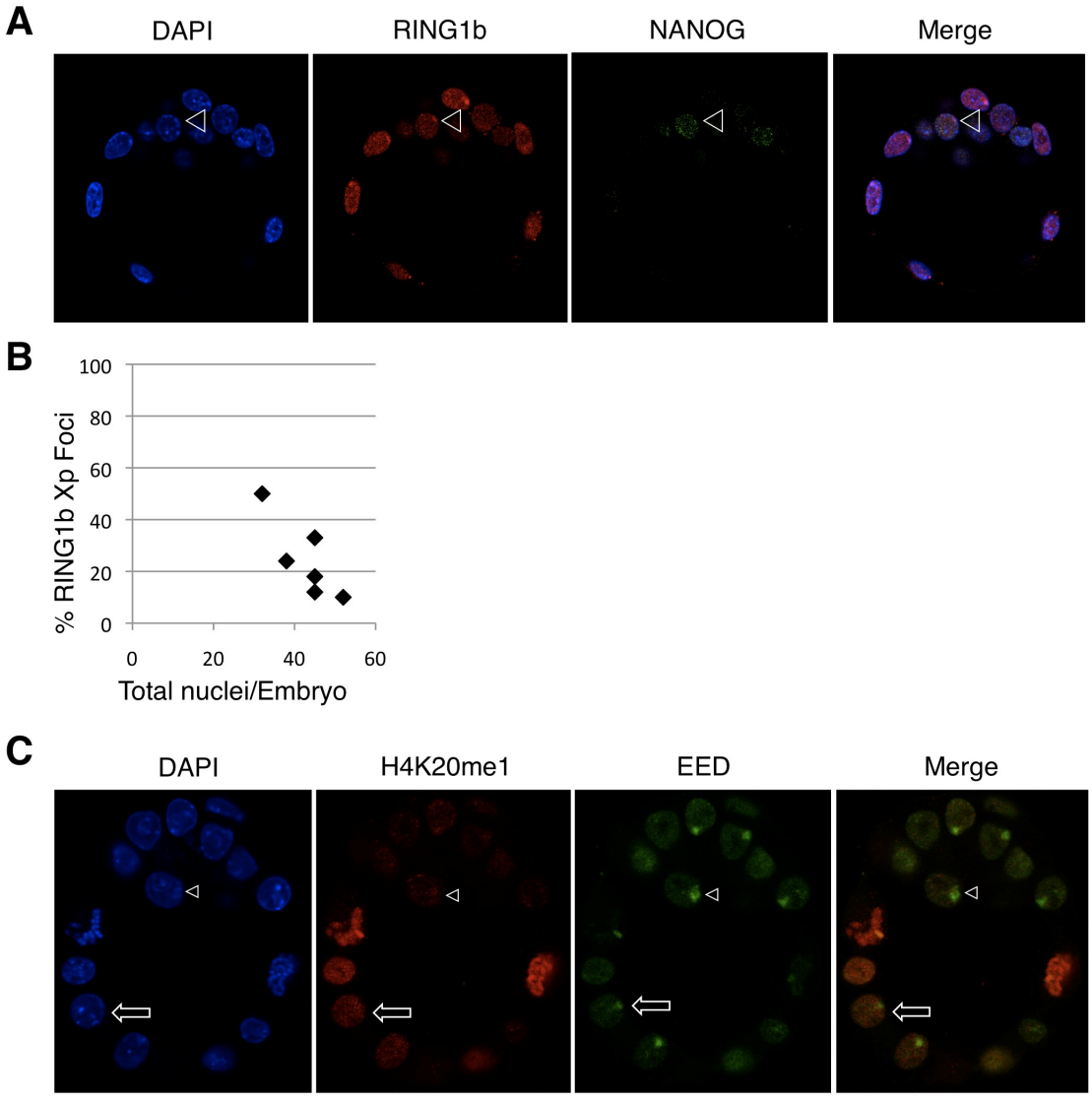

Figure 14 Characterization of XCI-associated epigenetic marks in mid-stage blastocysts.

(A) Immunostaining for RING1b (red, second panel) and NANOG (green, third panel). RING1b is found to accumulate on the Xp (arrow) in a NANOG positive ICM nucleus. (C) Despite localization of RING1b to the Xp in some mid-stage blastocyst nuclei, on average 25% of total cells in the embryo exhibited Xp RING1b foci. (D) H4K20me1 (red, second panel) and EED (green, third panel) immunostaining in mid-stage blastocyst. EED foci (green, third panel) mark the Xp in each nucleus. An arrowhead marks a nucleus where the Xp has H4K20me1. In contrast, an arrow marks a nucleus that does not exhibit H4K20me1 staining on the Xp.

coating and PRC2/H3K27me3 are removed. These results in the mid-stage ICM are consistent with maintenance of X-linked gene silencing after the loss of *Xist* expression during X-chromosome reactivation in female mouse germ cell development (Sugimoto and Abe, 2007). From these data, I argue that genic reactivation in the ICM is not simply a consequence of loss of *Xist* coating. Taking into account the findings in both chapter 3 and chapter 4, I propose that reprogramming of imprinted XCI requires two separable events: The first step, relief of Xp-linked gene repression, occurs between the early to mid-stage of ICM development and results in two active Xs at the mid-stage. The second step, extinction of Xp-*Xist* coating, occurs in late-stage ICMs by reprogramming of the Xp-*Xist* locus to suppress Xp-*Xist* expression. Together, genic reactivation and *Xist* reprogramming reset both X-chromosomes for initiation of random XCI in the epiblast. The results presented here are the first to report maintenance of imprinted gene silencing in the absence of Xp-*Xist* coating. These data suggest that Xp-linked gene silencing involves unknown mechanisms, which are independent of the presence of the *Xist* coat.

It is hypothesized that transcription factors that mediate pluripotency, particularly *Nanog*, directly couple X-chromosome reactivation to acquisition of ground-state pluripotency. In support of this hypothesis, it is reported that NANOG directly binds *Xist* intron 1, represses *Xist* expression in undifferentiated mouse ES cells, and prevents *Xist* coating (Navarro et al., 2008). Our study provides *in vivo* support for and expands on the role of NANOG in reprogramming XCI. Reprogramming in the ICM has been divided into *Nanog*-independent and *Nanog*-dependent phases (Silva et al., 2009). I pinpoint genic reactivation to the mid-stage ICM, which is prior to upregulation of *Nanog* expression and the defined phase of *Nanog*-dependent epigenetic remodeling. Therefore, I conclude that

initiation of genic reactivation is coupled to an early step in genome-wide reprogramming, which is independent of NANOG. This conclusion is supported by our observations that increased NANOG throughout the ICM did not result in increased Xp-linked gene reactivation.

In Chapter 2 and Chapter 3, I showed that the presence of NANOG, at the levels present in the early and mid-stage ICM, did not result in loss of Xp-*Xist* coating, which would appear inconsistent with the *Xist* gene as a direct target of NANOG repression. Female mouse epiblast stem cells (EpiSCs) also maintain *Xist* coating despite the presence of NANOG (Tesar et al., 2007). Interestingly, EpiSCs express lower levels of *Nanog* than ES cells, and it was shown that overexpression of *Nanog* in EpiSCs led to loss of inactive-X H3K27me3 enrichment (Silva et al., 2009). I show that ectopic upregulation of NANOG in *Grb2* -/- mid-stage ICMs forces premature loss of the Xp-*Xist* domain. The ability of NANOG to suppress *Xist* expression, therefore, likely depends on the dosage of NANOG. Dosage sensitivity in NANOG function may explain why depletion of Xp-*Xist* coating occurs after Xp-linked gene reactivation, in late ICMs and coincident with NANOG upregulation. Alternatively, the data presented here cannot rule out the possibility that Xp-*Xist* repression requires reprogramming factors in addition to NANOG, which are not present in early ICMs, mid-ICMs, or EpiSCs.

E) Materials and Methods

Embryo collection and Immunosurgery

Embryos were collected and immunosurgery were performed as previously described. Mice carrying a null mutation in *Grb2*$^{-/-}$ (GrmtmPaw2) were obtained from Tony Pawson

(University of Toronto, Canada) (Cheng et al., 1998). *Grb2*$^{+/-}$ females were crossed CD1 males carrying the X-GFP (D4.EGFP) transgene (Hadjantonakis et al., 1998). From these crosses, *Grb2*$^{+/-}$*; X*-GFP males were generated. Timed matings were performed with *Grb2*$^{+/-;}$ *X*-GFP males and *Grb2*$^{+/-}$ females. Preimplantation embryos were collected according to the procedures described in previous chapters and females were distinguished from males based on the presence of GFP. *Grb2*$^{+/-}$ blastocysts and ICMs were distinguished from littermate controls (*Grb2*$^{+/+}$ and *Grb2*$^{+/-}$) based on the upregulation of *Nanog* expression and down regulation of *Gata6* expression in the ICM. *Nanog* expression is unchanged in *Grb2*$^{-/-}$ 8-cell stage embryos, but I expect 12.5% of the embryos generated from this cross to be *Grb2*$^{-/-}$ and female. Therefore, when performing analysis 8-cell stage embryos four different litters were analyzed; mean number of embryos generated was 9 with approximately 50% of the embryos scoring GFP positive.

Immunostaining

Protocols for immunostaining were described in Chapter 2. Primary antibodies were Nanog (Chemicon, 1:1000), Cdx2 (Biogenex, 1:200), Gata6 (R&D Systems 1:1000), H3K27me3 (Upstate, 1:250), H4K20me1 (Upstate, 1:100), Ring1b (Arie Otte, Slater Institute, Amsterdam, The Netherlands, 1:50), SmcHD1 (1:200), Atrx (1:100), and EED (Arie Otte, Slater Institute, Amsterdam, The Netherlands, 1:100)

Chapter 5: Discussion

A) Preliminary results, *Xist* coating in Initiation of Random XCI

XCI is the conserved method of female dosage compensation from marsupials to eutherians. Interestingly, marsupial imprinted XCI occurs in the absence of the *Xist* gene, as the non-coding RNA is thought to have evolved *de novo* in eutherians from the pseudogenization of a protein-coding gene *Lnx3* (Duret et al., 2006). Unlike *Xist*, *Lnx3* expression is not sex-specific and has no defined role in marsupial imprinted XCI. Other features of XCI are shared, such as the enrichment of H3K27me3 at the Xi domain, although the abundance of H3K27me3 and, in turn, Xp silencing is less stable in marsupials (Chaumeil et al., 2011; Mahadevaiah et al., 2009).

Another example of *Xist*-independent silencing of X-chromosome sequence is meiotic sex chromosome inactivation (MSCI), the silencing of the unpaired X- and Y-chromosomes during male meiosis (Turner et al., 2002). The possibility exists that initiation of imprinted XCI, both in the mouse preimplantation embryo and marsupials, is achieved through inheritance of MSCI-mechanisms, such as still unidentified chromatin modifications placed on the Xp during spermatogenesis, predisposing the Xp for silencing (Namekawa et al., 2010). Here, I present preliminary data addressing the role of *Xist* coating in the initiation of random XCI. I argue that if in random XCI, which occurs *de novo* in the epiblast, Xi gene silencing can also be uncoupled from *Xist* coating*;* an attractive hypothesis

would be that *Xist*-independent initiation of X-linked gene silencing is generally conserved in the XCI process, from marsupial to eutherian.

Fundamentally, random XCI differs from imprinted XCI in that initiation of random XCI requires a choice step. Choice during imprinted XCI is 'locked'; the Xp is always the inactive chromosome, regardless of X-chromosome ploidy (Thornhill and Burgoyne, 1993). Consequently, in extraembryonic tissues, the Xm is active, and embryos that inherit a maternal *Xist* mutation are viable and undergo normal imprinted XCI. In contrast, the number of X-chromosomes that will be inactivated during random XCI is determined relative to the ploidy of the cell (Rastan and Robertson, 1985). Random XCI is initiated when the number of X-chromosomes exceeds one in a diploid nucleus. Each cell then makes the epigenetic choice to keep one X-chromosome active and to inactivate all supernumerary X-chromosomes.

Two different targeted deletions of the *Xist* gene have led to nonrandom XCI. Deletion of the *Xist* promoter through part of exon 1 results in what the authors concluded as secondary nonrandom XCI due to post-choice selection (Penny et al., 1996). These authors suggest that both WT and *Xist* mutant X-chromosomes can be chosen for silencing, but the choice of a mutated X-chromosome is lethal. These cells fail to inactivate the mutant X-chromosome and undergo post-choice selection, such that they are depleted during development. These authors concluded that *Xist* is required for initiation of random XCI; however, from their data it is unclear if defective silencing occurred due to defects in initiation or maintenance.

Another targeted deletion leaves the *Xist* promoter intact but spans from part of exon 1 through exon 5. This deletion also leads to nonrandom XCI, but the authors concluded that skewed XCI is due to altered choice, by primary nonrandom XCI (Nesterova et al., 2003; Newall et al., 2001). In this example, the *Xist* mutant X-chromosome was pre-empted from silencing because it was chosen as the active X-chromosome. Together, these data illustrate the difficulty in delineating the role of *Xist* coating in random XCI from loss of one *Xist* allele.

Panning and colleges subsequently revisited the mechanism of choice (Royce-Tolland et al., 2010). From their data, they determined that stochastic differences in the production of mature *Xist* transcripts underlie random choice. Prior to the onset of XCI, Xm and Xp *Xist* alleles both produce limited amounts of *Xist* transcripts. The noise inherent to low-levels of transcription results in subtle differences in the amount of mature *Xist* transcripts produced from Xm and Xp alleles. At the onset of XCI, these small differences are amplified and the X-chromosome that produced the most mature *Xist* transcripts is favored as the Xi. From this new model, it can be extrapolated that choice is set when both X-chromosomes are active, prior to initiation (Royce-Tolland et al., 2010). Thus, single *Xist* mutations cannot be used to determine if *Xist* is required for initiation of Xi gene silencing because the mutant X-chromosome is never selected for silencing in the first place.

Understanding whether *Xist* coating is necessary for silencing in random XCI requires generation of homozygous *Xist*-mutant female embryos, whereby both X-chromosomes have an equal chance to be chosen for silencing. I utilized a 21kb *Xist* deletion (XistΔ), encompassing 5kb upstream of the promoter through exon 3 (Csankovszki et al., 1999). Female embryos inheriting a paternal *Xist*Δ deletion (X^{WT}/XistΔ) exhibited 100% lethality

(Kalantry et al., 2009). In brief, X^{WT}/XistΔ females manifest growth retardation at E6.5, and uterine re-absorption occurs between E10.5 and E12.5. Random XCI initiates between E5.75 and E6.0; I hypothesized I could analyze random XCI in X^{WT}/XistΔ females because the initiation phase is prior to manifestation of the phenotype.

Next I generated homozygous *Xist*-mutant embryos by crossing heterozygous females (X^{WT}/XistΔ) with heterozygous males (XistΔ/Y). In this cross, 50% of the females are expected to be homozygous for the *Xist* mutant allele (XistΔ/XistΔ). Because the Xm is always active in extraembryonic tissues, XistΔ/XistΔ female embryos were not expected to display enhanced defects in the extraembryonic tissue development. However, XistΔ/XistΔ female embryos were not recovered at E6.5, despite evidence of implantation sites in decidua. Consistent with implantation into the uterus, XistΔ/XistΔ females could be recovered at E5.5. Gross analysis of the XistΔ/XistΔ morphology indicated that extraembryonic ectoderm was absent; conversely, these embryos contained a hollow space (Figure 15A). Extraembryonic ectoderm contains the trophectoderm stem cell population, and the absence of these cells may explain compromised development of XistΔ/XistΔ females, which are likely incapable of sustaining development of extraembryonic tissues. The surprising enhanced severity of XistΔ/XistΔ compared to X^{WT}/XistΔ is unresolved and could be a subject of future research.

In order to avoid the early implantation lethality found when female embryos maternally inherited a *Xist* mutation, I next utilized a conditional *Xist* allele (Xist2lox), which when recombined by CRE recombinase, removes sequence interior to the loxP sites. The

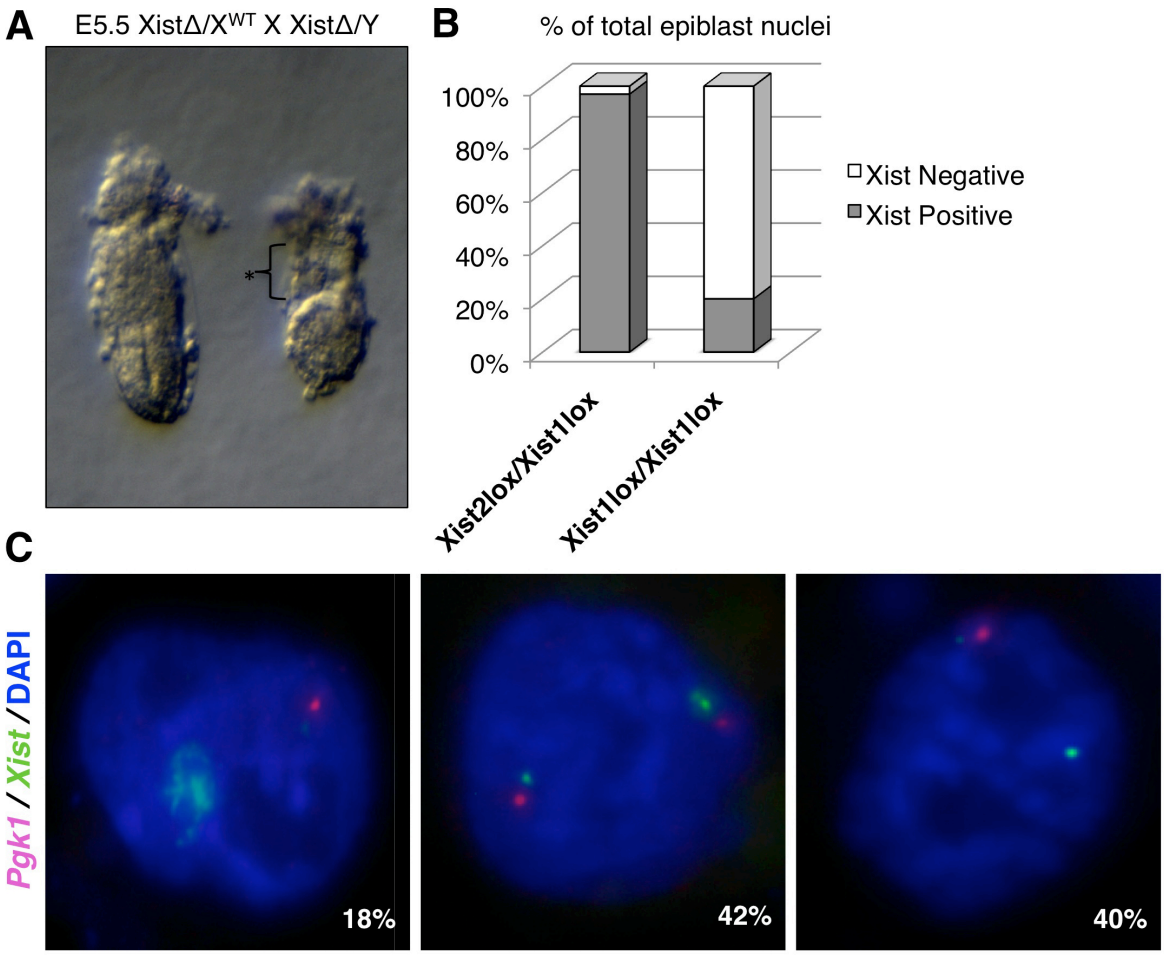

Figure 15 Epiblast cells exhibit Xi gene silencing in the absence of *Xist* coating.

(A) Representative E5.5 X^{WT}/XistΔ (right) and XistΔ/XistΔ (left) female embryos. The extraembryonic ectoderm cells are absent in the XistΔ/XistΔ. Brackets mark a hollow space where these cells should reside. **(B)** A RNA FISH probe that detects *Xist* and *Tsix* RNAs was used to determine the efficiency of CRE-mediated recombination for the Xist2lox allele. The distribution of *Xist* coating positive and *Xist* coating negative cells are graphed as a percentage of total epiblast cells. Xist1lox/Xist1lox embryos were Sox2cre positive. **(C)** Epiblast cells were isolated from Sox2cre positive embryos at E6.5. RNA FISH was performed using probes for *Pgk1* (red) and *Xist/Tsix* (green). The percentage of cells that were scored for each class, *Xist* coating/monoallelic (left panel), no *Xist* coating/biallelic (middle panel), and no *Xist* coating/monoallelic (right panel) are provided in the bottom corner of each image.

loxP sites in the Xist2lox allele are located 5kb upstream of the *Xist* promoter and within exon 3 (Csankovszki et al., 1999). I mated Xist2lox/Xist2lox females with Xist1lox/Y that also carry the *Sox2cre* transgene (Hayashi et al., 2002). From these matings, all female embryos inherited a mutated Xp-*Xist* allele; in contrast, only female embryos that inherit the *Sox2cre* will lack *Xist* expression from both X-chromosomes (Xist1lox/Xist1lox) in the epiblast. Utilizing this mating strategy, I recovered Xist1lox/Xist1lox at E6.5 that phenocopied X^{WT}/XistΔ females.

I used a RNA FISH probe that detects both *Xist* and *Tsix* to determine the degree of *Xist* coating found in Xist1lox/Xist1lox (n=4 epiblast) and Xist2lox/Xist1lox epiblast (n=6 epiblast) at E6.5. In these experiments, *Tsix* marks X-chromosomes that have failed to generate a *Xist* coat, locating both X-chromosomes in the nuclei. I show that approximately 18% of all epiblast cells in the *Sox2cre* positive female embryos exhibited *Xist* coating. This contrast Xist2lox/Xist1lox embryos where *Xist* coating was detected in 90% of epiblast cells (Figure 15B). The presence of *Xist* coating in a minority of Xist1lox/Xist1lox epiblast cells serves as a positive control for initiation of random XCI, indicating that Xist1lox/Xist1lox embryos are not delayed in epiblast development. By next combining RNA FISH probes for the X-linked gene *Pgk1* and *Xist/Tsix*, I analyzed X-linked gene silencing at E6.5. Of the 82% of Xist1lox/Xist1lox epiblast cells that did not have *Xist* coating, 42% of cells were biallelic for *Pgk1* expression. Remarkably, 40% of epiblast cells exhibited monoallelic *Pgk1* expression (Figure 15C). The presence of monoallelic nuclei is indicative of X-linked gene silencing. Although suggestive, these data imply that random XCI can occur in the absence of *Xist* coating, but more X-linked genes will need to be analyzed for definitive proof. Mouse has been the primary model organism to study eutherian XCI. Analysis of several

placental mammals now indicate diverse patterns of *Xist* RNA expression and coating during the initiation stage of XCI, consistent with our conclusion that initiation of random Xi gene silencing is uncoupled from *Xist* coating (Okamoto et al., 2011).

B) Future Directions

1. Identifying X-linked sequences that regulate initiation of XCI

Here, I present preliminary observations that extend *Xist*-independent XCI processes to random XCI. If these observations can be reproduced for multiple X-linked genes, then they would challenge that long held hypothesized that XCI in marsupials and eutherians is mechanistically different (Chaumeil et al., 2011). As discussed in the introductory chapters, phylogenetic comparisons have shown that differentiation of the X- and Y-chromosomes did not occur as a single event. Genes on the proto-Y degenerated individually, or regionally; likewise, compensatory dosage compensation in females probably evolved in a piecemeal fashion, with XCI mechanisms gradually encompassing segments of the X-chromosome (Jegalian and Page, 1998). Thus, evolutionary studies are inconsistent with models that assume Xi transcriptional repression is a function of whole-chromosome topology. Evolutionary models are more consisted with Xi gene expression being determined by local or regional elements.

Mauro Calabrese has performed RNA-sequencing (RNA-Seq) in a panel of TS cells derived from crosses of *Castaneous* (CAST) to C57BL/6J (B6) mice. Using a strand-specific RNA-Seq protocol, single nucleotide polymorphisms (SNPs) between the two strains facilitated quantitative comparisons of Xa and Xi transcripts. From 260 genes for which high confidence allelic expression data was obtained, 223 genes were inactivated in TS cells;

whereas, 37 genes, depending on the genetic background, exhibited some degree of expression from the Xi (Calabrese et al.). These datasets have provided a useful tool to dissect mechanisms regulating X-linked gene expression. For example, motif analysis has identified DNA sequences that are putatively involved in regulating escape from XCI.

One research group has taken the approach of classifying a limited number of X-linked genes into early inactivators, late inactivators, and escapers (Patrat et al., 2009). High-resolution analysis of X-linked gene expression has not been performed during the initiation phase of XCI; RNA-seq performed on pools of preimplantation embryos may be useful in expanding on the number of X-linked genes classified as early inactivators, late inactivators, and escapers. Profiling X-chromosome-wide silencing kinetics may identify putative sequences that function as local regulators of X-linked gene transcriptional activity. I hypothesize early inactivating genes either contain, or exist near regulatory sequences that function as initiation points for silencing.

Repetitive non-coding sequences, particularly LINE-1 retrotransposons, have emerged as attractive facilitators of XCI, perhaps independent of *Xist* RNA (Chow et al., 2010; Namekawa et al., 2010). LINEs are therefore potential candidates for sequence that may focally regulate X-linked gene activity, consistent with a recent report in fission yeast (Tang et al., 2010; Zaratiegui et al., 2011). Cot-1 RNA FISH can be used to measure expression of repetitive sequences, including LINEs. I report that mid-stage ICMs are enriched, relative to trophectoderm and early ICMs, for nuclei exhibiting Cot-1 hybridization internal to the *Xist* domain, suggesting repetitive sequences exhibit reactivation prior to removal of *Xist* coating. One testable hypothesis would be that early inactivating genes are

in regions of high LINE density, with LINE silencing facilitating initiation, and consequently reactivation of X-linked genes during preimplantation development.

2. Is there mechanistic link between Xa upregulation and Xi silencing?

In mammals, research has focused on XCI, which achieves balance in X-linked gene expression between the sexes; however, a transcriptional balance is also achieved between X-chromosomes and autosomes (Cheng and Disteche, 2006; Lin et al., 2007). General transcription levels from active X-linked genes are elevated in both sexes to the relative level of genes expression on the pairs of homologous autosomes. How two-fold upregulation of active X-linked genes is achieved remains poorly understood. One hypothesis is that active-X upregulation and XCI are mechanistically linked. In support of this hypothesis, H3K27me3 deposition on Xi genes has been shown to be tightly associated with Xa transcription (Marks et al., 2009). Expanding on these observations, Mauro Calabrese performed allele-specific, high-resolution H3K27me3 ChIP-sequencing (ChIP-seq) in TS cells. H3K27me3 was observed at Xi genic sequence; both within transcription start sites (TSS) and gene bodies, but H3K27me3 was consistently higher at transcription start sites (TSSs) of inactivated genes. Genes that are not transcribed in TS cells did not exhibit H3K27me3 enrichment above average Xi levels. These ChIP-seq datasets indicate that some mechanisms of XCI may respond to transcription from the Xa. Consequently, exploring active X-upregulation could facilitate elucidation of XCI, providing a holistic understanding of mammalian dosage compensation mechanisms.

Control of transcription is regulated at multiple levels, including recruitment of RNA polymerase II and general transcription factors to the promoter, as well as initiation,

elongation, and termination of transcription. Dosage compensation of active X-chromosomes exist not only in mammals, but also in *Drosophila melanogaster*, where the single X-chromosome is upregulated two-fold in XY males (Gelbart and Kuroda, 2009). Global run-on sequencing (GRO-seq) in drosophila male cell lines has found that transcriptional upregulation occurs by enhanced transcriptional elongation at X-linked genes (Larschan et al., 2011). Using these experiments as a guide, allele-specific GRO-seq could be performed in mammalian cells, and the RNA Polymerase II pausing and elongation indexes for all expressed Xa genes determined. These Xa indexes then compared to autosomal gene average indexes (Core et al., 2008; Larschan et al., 2011). These methods, as described in Larschan et al., may address the unanswered question of if and how transcription of X-linked sequence differs from transcription on autosomes. Likewise, these methods may also address the unanswered question of what step in transcription is first blocked during the initiation phase of Xi gene repression.

The Male-specific lethal (MSL) complex regulates dosage compensation in *Drosophila Melanogaster*. The MSL complex is made up of five proteins, including the histone acetyltransferase Males Absent on the First (MOF). MOF is responsible for acetylating histone 4 at lysine 16 (H4K16Ac), a chromatin modification that promotes transcriptional elongation by releasing RNA Polymerase II from pausing at promoters (Kapoor-Vazirani et al., 2011). Consistent with a role in regulating transcriptional elongation, a 3' bias of H4K16Ac is a distinctive characteristic of dosage compensated X-linked genes in *Drosophila melanogaster (Gelbart et al., 2009; Kind et al., 2008)*. At present, it is unknown if chromatin of the Xa in mammals differs in anyway from that of autosomes; however, connecting upregulation and XCI mechanisms, H3K27me3 has been

proposed to prevent transcriptional elongation. As a first step in examining Xa chromatin, CHIP-seq analysis of H4K16Ac could be used to determine if a similar 3' bias of H4K16Ac is present at transcribed Xa genes in mammalian cells. In combination with GRO-seq, the proposed experiments may lead the way in outlining a putative mechanism for Xa dosage compensation.

C) Concluding Remarks

The experiments described in these chapters are supported by observations of Sundeep Kalantry, a former college, that paternal-*Xist* mutant (X^{WT}/XistΔ) embryos transiently initiate Xp silencing at the 8-cell stage, but at post-implantation the Xp variably reactivated in extraembryonic tissues (Kalantry et al., 2009). These X^{WT}/XistΔ embryos phenocopied the developmental defects described in female embryos carrying an EED mutation, a complementation that is expected if *Xist* RNA directly recruits PRC2 (Kalantry et al., 2006; Wang et al., 2001; Zhao et al., 2010). Based on these observations, I confer that *Xist* coating likely behaves as a molecular scaffold, recruiting H3K27me3 and other epigenetic modifications to the Xi and initiating folding of the Xi chromosome territory into a conformation that is repressive for transcriptional machinery.

However, the data presented here call into question the requirement for *Xist* coating and H3K27me3 during the earliest phase of XCI; suggestive that large-scale chromatin remodeling is not sufficient to determine Xi gene expression patterns. These observations are inconsistent with a role for *Xist* RNA as the sole initiator of XCI, arguing against the repressive compartment model for initiation of genic silencing. I suggest alternatively that XCI in placental mammals has many layers of epigenetic modification, with as-of-yet unidentified mechanisms determining Xi gene silencing at the regional, or local level. This

alternative idea is consistent with a chromosome-conformation capture-on-chip (4C) study that separates *Xist*-dependent Xi chromosome conformation from X-linked gene transcriptional activity (Splinter et al., 2011). The locally determined mechanism is likely conserved from marsupial to eutherian; conversely, *Xist* evolved in eutherians to increase the efficiency of Xi silencing, supporting site-specific regulatory mechanisms and augmenting stable recruitment of chromatin modifications. Both layers of epigenetic modification are probably necessary in differentiated cells for stable maintenance of XCI. But at the earliest phases of the XCI process, such as in the ICM, locally regulated Xi gene silencing is primary to *Xist* dependent heterochromatinization, perhaps because chromosome-wide changes take several cell divisions to develop, explaining the *Xist*-independent reactivation we have identified here.

I began these experiments interested in the association of cell potency and X-chromosome programming. I conclude that XCI robustly initiates in the totipotent cells of the preimplantation embryo; genic inactivation and reactivation is independent of NANOG. These data suggest that there is no clear distinction between X-linked gene activity and the pluripotent state. But rather my data support a direct link between pluripotency-associated transcription factors and *Xist* RNA. *In vivo* NANOG levels can regulate *Xist* expression, corroborating previous *ex vivo* results (Navarro et al., 2008). These data suggest that X-chromosome reactivation is not simply a reversal of *Xist* coating, highlighting how little we know about the epigenetic reprogramming of XCI. I caution that given this complexity, X-chromosome activation may not be the best indicator of pluripotency, such as it is currently utilized in mouse and human ES cell models.

XCI is an established paradigm in the study of epigenetic mechanisms that is often examined in *ex vivo* contexts. By focusing on *in vivo* reactivation in the ICM, I gained novel insight into mechanisms of XCI. In combination with other work from this laboratory, our perception of the XCI process and the possible role of non-coding RNAs throughout the genome have been altered. We are left with many unanswered questions, setting the stage for future exploration into undiscovered factors and highlighting the importance of DNA sequence to the mechanisms that determine transcriptional activity of X-linked genes.

C) Methods

Mouse Strains

Mice were maintained on a mixed background. The Xist2lox conditional allele was described (Csankovszki et al., 1999). The Sox2-cre transgene was previously described (Hayashi et al., 2002). In order to generate XistΔ animals, I mated WT females that carried a Zp3-cre transgene with Xist2lox/Y males to generate X^{WT}/Xist2lox; Zp3-cre/+ females (Lewandoski et al., 1997). In the following generation, X^{WT}/Xist2lox; Zp3-cre/+ females were mated with Xist2lox/Y males to generate X^{WT}/Xistlox females and Xist1lox/Y males. At this point, the Zp3-cre was bred out of the colony. Xist1lox was from then referred to as XistΔ because the sequence encompassed by the loxP sites had been permanently recombined out. In order to maintain the colony, X^{WT}/XistΔ were mated to WT males that carried the X-GFP allele (Hadjantonakis et al., 1998). From these crosses, I generated X^{WT}/XistΔ-GFP females. X^{WT}/XistΔ-GFP females were then mated to CD1 males to generate X^{WT}/XistΔ females and XistΔ-GFP/Y males.

Embryo Dissections

Whole embryos were dissected in PBS plus 6mg/ml BSA at room temperature (serum is to prevent stickiness). After embryos were dissected out of the deciduas, genotyping was performed by lysing entire embryos or micro-dissected embryonic tissue in 50μl of Tail Lysis Buffer (50mM Tris pH8.8, 1mM EDTA, and 0.5% Tween) with 200μg/ml of Proteinase K. For RNA FISH on epiblast cells, the epiblast was micro-dissected after whole embryo dissection. To micro-dissect the epiblast, the dissection was performed on glass slides. Glass is used to prevent the embryo from sticking to the surface. A thinly pulled

capillary was used to split the embryo at the embryonic and extraembryonic junction into two parts. The extraembryonic parts were used to genotype the embryos.

From the embryonic part, I used forceps to carefully remove the embryonic visceral endoderm from the epiblast. Epiblast cells were then incubated in 0.05% trypsin to breakup the tissue into small cell clumps. In more detail, the 0.05% trypsin was pre-warmed to 37°C, and epiblast cells were placed in 50μl drops of 0.05% trypsin. A mouth pipette was used to carefully draw the epiblast up and down. Eventually, the epiblast would breakup into small clumps. The entire process would take less than 1 minute. Small cell clumps were then transferred to M2 plus 10% fetal bovine serum to neutralize the trypsin. From this point on RNA FISH was performed as for the ICMs described in Chapter 1. The *Pgk1* FISH probe was previously described in (Kalantry et al., 2006)

Bibliography

Agrelo, R., Souabni, A., Novatchkova, M., Haslinger, C., Leeb, M., Komnenovic, V., Kishimoto, H., Gresh, L., Kohwi-Shigematsu, T., Kenner, L. et al. (2009). SATB1 defines the developmental context for gene silencing by Xist in lymphoma and embryonic cells. *Dev Cell* **16**, 507-16.

Agulnik, A. I., Mitchell, M. J., Mattei, M. G., Borsani, G., Avner, P. A., Lerner, J. L. and Bishop, C. E. (1994). A novel X gene with a widely transcribed Y-linked homologue escapes X-inactivation in mouse and human. *Hum Mol Genet* **3**, 879-84.

Ahmed, K., Dehghani, H., Rugg-Gunn, P., Fussner, E., Rossant, J. and Bazett-Jones, D. P. (2010). Global chromatin architecture reflects pluripotency and lineage commitment in the early mouse embryo. *PLoS One* **5**, e10531.

Berg, D. K., van Leeuwen, J., Beaumont, S., Berg, M. and Pfeffer, P. L. (2010). Embryo loss in cattle between Days 7 and 16 of pregnancy. *Theriogenology* **73**, 250-60.

Bernstein, B. E., Mikkelsen, T. S., Xie, X., Kamal, M., Huebert, D. J., Cuff, J., Fry, B., Meissner, A., Wernig, M., Plath, K. et al. (2006). A bivalent chromatin structure marks key developmental genes in embryonic stem cells. *Cell* **125**, 315-26.

Bischoff, M., Parfitt, D. E. and Zernicka-Goetz, M. (2008). Formation of the embryonic-abembryonic axis of the mouse blastocyst: relationships between orientation of early cleavage divisions and pattern of symmetric/asymmetric divisions. *Development* **135**, 953-62.

Blewitt, M. E., Gendrel, A. V., Pang, Z., Sparrow, D. B., Whitelaw, N., Craig, J. M., Apedaile, A., Hilton, D. J., Dunwoodie, S. L., Brockdorff, N. et al. (2008). SmcHD1, containing a structural-maintenance-of-chromosomes hinge domain, has a critical role in X inactivation. *Nat Genet* **40**, 663-9.

Boyer, L. A., Lee, T. I., Cole, M. F., Johnstone, S. E., Levine, S. S., Zucker, J. P., Guenther, M. G., Kumar, R. M., Murray, H. L., Jenner, R. G. et al. (2005). Core transcriptional regulatory circuitry in human embryonic stem cells. *Cell* **122**, 947-56.

Boyer, L. A., Plath, K., Zeitlinger, J., Brambrink, T., Medeiros, L. A., Lee, T. I., Levine, S. S., Wernig, M., Tajonar, A., Ray, M. K. et al. (2006). Polycomb complexes repress developmental regulators in murine embryonic stem cells. *Nature* **441**, 349-53.

Brockdorff, N., Ashworth, A., Kay, G. F., McCabe, V. M., Norris, D. P., Cooper, P. J., Swift, S. and Rastan, S. (1992). The product of the mouse Xist gene is a 15 kb inactive X-specific transcript containing no conserved ORF and located in the nucleus. *Cell* **71**, 515-26.

Brown, C. J., Ballabio, A., Rupert, J. L., Lafreniere, R. G., Grompe, M., Tonlorenzi, R. and Willard, H. F. (1991). A gene from the region of the human X inactivation centre is expressed exclusively from the inactive X chromosome. *Nature* **349**, 38-44.

Cauffman, G., Van de Velde, H., Liebaers, I. and Van Steirteghem, A. (2005). Oct-4 mRNA and protein expression during human preimplantation development. *Mol Hum Reprod* **11**, 173-81.

Chaumeil, J., Le Baccon, P., Wutz, A. and Heard, E. (2006). A novel role for Xist RNA in the formation of a repressive nuclear compartment into which genes are recruited when silenced. *Genes Dev* **20**, 2223-37.

Chaumeil, J., Okamoto, I., Guggiari, M. and Heard, E. (2002). Integrated kinetics of X chromosome inactivation in differentiating embryonic stem cells. *Cytogenet Genome Res* **99**, 75-84.

Chaumeil, J., Waters, P. D., Koina, E., Gilbert, C., Robinson, T. J. and Graves, J. A. (2011). Evolution from XIST-independent to XIST-controlled X-chromosome inactivation: epigenetic modifications in distantly related mammals. *PLoS One* **6**, e19040.

Chazaud, C., Yamanaka, Y., Pawson, T. and Rossant, J. (2006). Early lineage segregation between epiblast and primitive endoderm in mouse blastocysts through the Grb2-MAPK pathway. *Dev Cell* **10**, 615-24.

Cheng, A. M., Saxton, T. M., Sakai, R., Kulkarni, S., Mbamalu, G., Vogel, W., Tortorice, C. G., Cardiff, R. D., Cross, J. C., Muller, W. J. et al. (1998). Mammalian Grb2 regulates multiple steps in embryonic development and malignant transformation. *Cell* **95**, 793-803.

Cheng, M. K. and Disteche, C. M. (2006). A balancing act between the X chromosome and the autosomes. *J Biol* **5**, 2.

Chiba, H., Hirasawa, R., Kaneda, M., Amakawa, Y., Li, E., Sado, T. and Sasaki, H. (2008). De novo DNA methylation independent establishment of maternal imprint on X chromosome in mouse oocytes. *Genesis* **46**, spc one.

Chong, S., Vickaryous, N., Ashe, A., Zamudio, N., Youngson, N., Hemley, S., Stopka, T., Skoultchi, A., Matthews, J., Scott, H. S. et al. (2007). Modifiers of epigenetic reprogramming show paternal effects in the mouse. *Nat Genet* **39**, 614-22.

Chow, J. C., Ciaudo, C., Fazzari, M. J., Mise, N., Servant, N., Glass, J. L., Attreed, M., Avner, P., Wutz, A., Barillot, E. et al. (2010). LINE-1 activity in facultative heterochromatin formation during X chromosome inactivation. *Cell* **141**, 956-69.

Clemson, C. M., McNeil, J. A., Willard, H. F. and Lawrence, J. B. (1996). XIST RNA paints the inactive X chromosome at interphase: evidence for a novel RNA involved in nuclear/chromosome structure. *J Cell Biol* **132**, 259-75.

Cooke, H. J., Brown, W. R. and Rappold, G. A. (1985). Hypervariable telomeric sequences from the human sex chromosomes are pseudoautosomal. *Nature* **317**, 687-92.

Core, L. J., Waterfall, J. J. and Lis, J. T. (2008). Nascent RNA sequencing reveals widespread pausing and divergent initiation at human promoters. *Science* **322**, 1845-8.

Corry, G. N., Tanasijevic, B., Barry, E. R., Krueger, W. and Rasmussen, T. P. (2009). Epigenetic regulatory mechanisms during preimplantation development. *Birth Defects Res C Embryo Today* **87**, 297-313.

Csankovszki, G., Panning, B., Bates, B., Pehrson, J. R. and Jaenisch, R. (1999). Conditional deletion of Xist disrupts histone macroH2A localization but not maintenance of X inactivation. *Nat Genet* **22**, 323-4.

De La Fuente, R., Hahnel, A., Basrur, P. K. and King, W. A. (1999). X inactive-specific transcript (Xist) expression and X chromosome inactivation in the preattachment bovine embryo. *Biol Reprod* **60**, 769-75.

de Napoles, M., Mermoud, J. E., Wakao, R., Tang, Y. A., Endoh, M., Appanah, R., Nesterova, T. B., Silva, J., Otte, A. P., Vidal, M. et al. (2004). Polycomb group proteins Ring1A/B link ubiquitylation of histone H2A to heritable gene silencing and X inactivation. *Dev Cell* **7**, 663-76.

Deakin, J. E., Chaumeil, J., Hore, T. A. and Marshall Graves, J. A. (2009). Unravelling the evolutionary origins of X chromosome inactivation in mammals: insights from marsupials and monotremes. *Chromosome Res* **17**, 671-85.

Dietrich, J. E. and Hiiragi, T. (2007). Stochastic patterning in the mouse pre-implantation embryo. *Development* **134**, 4219-31.

Duret, L., Chureau, C., Samain, S., Weissenbach, J. and Avner, P. (2006). The Xist RNA gene evolved in eutherians by pseudogenization of a protein-coding gene. *Science* **312**, 1653-5.

Dvash, T., Lavon, N. and Fan, G. (2010). Variations of X chromosome inactivation occur in early passages of female human embryonic stem cells. *PLoS One* **5**, e11330.

Epstein, C. J. (1969). Mammalian oocytes: X chromosome activity. *Science* **163**, 1078-9.

Ferguson-Smith, A. C. and Surani, M. A. (2001). Imprinting and the epigenetic asymmetry between parental genomes. *Science* **293**, 1086-9.

Garrick, D., Sharpe, J. A., Arkell, R., Dobbie, L., Smith, A. J., Wood, W. G., Higgs, D. R. and Gibbons, R. J. (2006). Loss of Atrx affects trophoblast development and the pattern of X-inactivation in extraembryonic tissues. *PLoS Genet* **2**, e58.

Gartler, S. M. and Riggs, A. D. (1983). Mammalian X-chromosome inactivation. *Annu Rev Genet* **17**, 155-90.

Gelbart, M. E. and Kuroda, M. I. (2009). Drosophila dosage compensation: a complex voyage to the X chromosome. *Development* **136**, 1399-410.

Gelbart, M. E., Larschan, E., Peng, S., Park, P. J. and Kuroda, M. I. (2009). Drosophila MSL complex globally acetylates H4K16 on the male X chromosome for dosage compensation. *Nat Struct Mol Biol* **16**, 825-32.

Goto, Y. and Takagi, N. (1998). Tetraploid embryos rescue embryonic lethality caused by an additional maternally inherited X chromosome in the mouse. *Development* **125**, 3353-63.

Graves, J. A. (2010). Review: Sex chromosome evolution and the expression of sex-specific genes in the placenta. *Placenta* **31 Suppl**, S27-32.

Hadjantonakis, A. K., Gertsenstein, M., Ikawa, M., Okabe, M. and Nagy, A. (1998). Non-invasive sexing of preimplantation stage mammalian embryos. *Nat Genet* **19**, 220-2.

Hall, L. L., Byron, M., Butler, J., Becker, K. A., Nelson, A., Amit, M., Itskovitz-Eldor, J., Stein, J., Stein, G., Ware, C. et al. (2008). X-inactivation reveals epigenetic anomalies in most hESC but identifies sublines that initiate as expected. *J Cell Physiol* **216**, 445-52.

Hall, L. L., Byron, M., Sakai, K., Carrel, L., Willard, H. F. and Lawrence, J. B. (2002). An ectopic human XIST gene can induce chromosome inactivation in postdifferentiation human HT-1080 cells. *Proc Natl Acad Sci U S A* **99**, 8677-82.

Hamazaki, T., Kehoe, S. M., Nakano, T. and Terada, N. (2006). The Grb2/Mek pathway represses Nanog in murine embryonic stem cells. *Mol Cell Biol* **26**, 7539-49.

Hayashi, S., Lewis, P., Pevny, L. and McMahon, A. P. (2002). Efficient gene modulation in mouse epiblast using a Sox2Cre transgenic mouse strain. *Mech Dev* **119 Suppl 1**, S97-S101.

Huynh, K. D. and Lee, J. T. (2003). Inheritance of a pre-inactivated paternal X chromosome in early mouse embryos. *Nature* **426**, 857-62.

Jegalian, K. and Page, D. C. (1998). A proposed path by which genes common to mammalian X and Y chromosomes evolve to become X inactivated. *Nature* **394**, 776-80.

Kalantry, S., Mills, K. C., Yee, D., Otte, A. P., Panning, B. and Magnuson, T. (2006). The Polycomb group protein Eed protects the inactive X-chromosome from differentiation-induced reactivation. *Nat Cell Biol* **8**, 195-202.

Kalantry, S., Purushothaman, S., Bowen, R. B., Starmer, J. and Magnuson, T. (2009). Evidence of Xist RNA-independent initiation of mouse imprinted X-chromosome inactivation. *Nature* **460**, 647-51.

Kaneda, M., Okano, M., Hata, K., Sado, T., Tsujimoto, N., Li, E. and Sasaki, H. (2004). Essential role for de novo DNA methyltransferase Dnmt3a in paternal and maternal imprinting. *Nature* **429**, 900-3.

Kapoor-Vazirani, P., Kagey, J. D. and Vertino, P. M. (2011). SUV420H2-mediated H4K20 trimethylation enforces RNA polymerase II promoter-proximal pausing by blocking hMOF-dependent H4K16 acetylation. *Mol Cell Biol* **31**, 1594-609.

Kay, G. F., Penny, G. D., Patel, D., Ashworth, A., Brockdorff, N. and Rastan, S. (1993). Expression of Xist during mouse development suggests a role in the initiation of X chromosome inactivation. *Cell* **72**, 171-82.

Kelley, R. L., Solovyeva, I., Lyman, L. M., Richman, R., Solovyev, V. and Kuroda, M. I. (1995). Expression of msl-2 causes assembly of dosage compensation regulators on the X chromosomes and female lethality in Drosophila. *Cell* **81**, 867-77.

Kind, J., Vaquerizas, J. M., Gebhardt, P., Gentzel, M., Luscombe, N. M., Bertone, P. and Akhtar, A. (2008). Genome-wide analysis reveals MOF as a key regulator of dosage compensation and gene expression in Drosophila. *Cell* **133**, 813-28.

Kobolak, J., Kiss, K., Polgar, Z., Mamo, S., Rogel-Gaillard, C., Tancos, Z., Bock, I., Baji, A. G., Tar, K., Pirity, M. K. et al. (2009). Promoter analysis of the rabbit POU5F1 gene and its expression in preimplantation stage embryos. *BMC Mol Biol* **10**, 88.

Kohlmaier, A., Savarese, F., Lachner, M., Martens, J., Jenuwein, T. and Wutz, A. (2004). A chromosomal memory triggered by Xist regulates histone methylation in X inactivation. *PLoS Biol* **2**, E171.

Ku, M., Koche, R. P., Rheinbay, E., Mendenhall, E. M., Endoh, M., Mikkelsen, T. S., Presser, A., Nusbaum, C., Xie, X., Chi, A. S. et al. (2008). Genomewide analysis of PRC1 and PRC2 occupancy identifies two classes of bivalent domains. *PLoS Genet* **4**, e1000242.

Lahn, B. T. and Page, D. C. (1999). Four evolutionary strata on the human X chromosome. *Science* **286**, 964-7.

Lanner, F. and Rossant, J. (2010). The role of FGF/Erk signaling in pluripotent cells. *Development* **137**, 3351-60.

Larschan, E., Bishop, E. P., Kharchenko, P. V., Core, L. J., Lis, J. T., Park, P. J. and Kuroda, M. I. (2011). X chromosome dosage compensation via enhanced transcriptional elongation in Drosophila. *Nature* **471**, 115-8.

Lee, J. T., Davidow, L. S. and Warshawsky, D. (1999). Tsix, a gene antisense to Xist at the X-inactivation centre. *Nat Genet* **21**, 400-4.

Lee, T. I., Jenner, R. G., Boyer, L. A., Guenther, M. G., Levine, S. S., Kumar, R. M., Chevalier, B., Johnstone, S. E., Cole, M. F., Isono, K. et al. (2006). Control of developmental regulators by Polycomb in human embryonic stem cells. *Cell* **125**, 301-13.

Lengner, C. J., Gimelbrant, A. A., Erwin, J. A., Cheng, A. W., Guenther, M. G., Welstead, G. G., Alagappan, R., Frampton, G. M., Xu, P., Muffat, J. et al. (2010). Derivation of pre-X inactivation human embryonic stem cells under physiological oxygen concentrations. *Cell* **141**, 872-83.

Lewandoski, M., Wassarman, K. M. and Martin, G. R. (1997). Zp3-cre, a transgenic mouse line for the activation or inactivation of loxP-flanked target genes specifically in the female germ line. *Curr Biol* **7**, 148-51.

Lin, H., Gupta, V., Vermilyea, M. D., Falciani, F., Lee, J. T., O'Neill, L. P. and Turner, B. M. (2007). Dosage compensation in the mouse balances up-regulation and silencing of X-linked genes. *PLoS Biol* **5**, e326.

Lyon, M. F. (1961). Gene action in the X-chromosome of the mouse (Mus musculus L.). *Nature* **190**, 372-3.

Lyon, M. F. (1998). X-chromosome inactivation: a repeat hypothesis. *Cytogenet Cell Genet* **80**, 133-7.

Mahadevaiah, S. K., Royo, H., VandeBerg, J. L., McCarrey, J. R., Mackay, S. and Turner, J. M. (2009). Key features of the X inactivation process are conserved between marsupials and eutherians. *Curr Biol* **19**, 1478-84.

Mak, W., Baxter, J., Silva, J., Newall, A. E., Otte, A. P. and Brockdorff, N. (2002). Mitotically stable association of polycomb group proteins eed and enx1 with the inactive x chromosome in trophoblast stem cells. *Curr Biol* **12**, 1016-20.

Mak, W., Nesterova, T. B., de Napoles, M., Appanah, R., Yamanaka, S., Otte, A. P. and Brockdorff, N. (2004). Reactivation of the paternal X chromosome in early mouse embryos. *Science* **303**, 666-9.

Marks, H., Chow, J. C., Denissov, S., Francoijs, K. J., Brockdorff, N., Heard, E. and Stunnenberg, H. G. (2009). High-resolution analysis of epigenetic changes associated with X inactivation. *Genome Res* **19**, 1361-73.

Mayer, W., Niveleau, A., Walter, J., Fundele, R. and Haaf, T. (2000). Demethylation of the zygotic paternal genome. *Nature* **403**, 501-2.

Mendenhall, E. M., Koche, R. P., Truong, T., Zhou, V. W., Issac, B., Chi, A. S., Ku, M. and Bernstein, B. E. (2010). GC-rich sequence elements recruit PRC2 in mammalian ES cells. *PLoS Genet* **6**, e1001244.

Mermoud, J. E., Popova, B., Peters, A. H., Jenuwein, T. and Brockdorff, N. (2002). Histone H3 lysine 9 methylation occurs rapidly at the onset of random X chromosome inactivation. *Curr Biol* **12**, 247-51.

Mietton, F., Sengupta, A. K., Molla, A., Picchi, G., Barral, S., Heliot, L., Grange, T., Wutz, A. and Dimitrov, S. (2009). Weak but uniform enrichment of the histone variant macroH2A1 along the inactive X chromosome. *Mol Cell Biol* **29**, 150-6.

Min, I. M., Waterfall, J. J., Core, L. J., Munroe, R. J., Schimenti, J. and Lis, J. T. (2011). Regulating RNA polymerase pausing and transcription elongation in embryonic stem cells. *Genes Dev* **25**, 742-54.

Moreira de Mello, J. C., de Araujo, E. S., Stabellini, R., Fraga, A. M., de Souza, J. E., Sumita, D. R., Camargo, A. A. and Pereira, L. V. (2010). Random X inactivation and extensive mosaicism in human placenta revealed by analysis of allele-specific gene expression along the X chromosome. *PLoS One* **5**, e10947.

Morey, C., Kress, C. and Bickmore, W. A. (2009). Lack of bystander activation shows that localization exterior to chromosome territories is not sufficient to up-regulate gene expression. *Genome Res* **19**, 1184-94.

Morgan, H. D., Santos, F., Green, K., Dean, W. and Reik, W. (2005). Epigenetic reprogramming in mammals. *Hum Mol Genet* **14 Spec No 1**, R47-58.

Muller, H. J. (1964). The Relation of Recombination to Mutational Advance. *Mutat Res* **106**, 2-9.

Nakamura, T., Arai, Y., Umehara, H., Masuhara, M., Kimura, T., Taniguchi, H., Sekimoto, T., Ikawa, M., Yoneda, Y., Okabe, M. et al. (2007). PGC7/Stella protects against DNA demethylation in early embryogenesis. *Nat Cell Biol* **9**, 64-71.

Namekawa, S. H., Payer, B., Huynh, K. D., Jaenisch, R. and Lee, J. T. Two-step imprinted X inactivation: repeat versus genic silencing in the mouse. *Mol Cell Biol* **30**, 3187-205.

Namekawa, S. H., Payer, B., Huynh, K. D., Jaenisch, R. and Lee, J. T. (2010). Two-step imprinted X inactivation: repeat versus genic silencing in the mouse. *Mol Cell Biol* **30**, 3187-205.

Navarro, P. and Avner, P. (2009). When X-inactivation meets pluripotency: an intimate rendezvous. *FEBS Lett* **583**, 1721-7.

Navarro, P., Chambers, I., Karwacki-Neisius, V., Chureau, C., Morey, C., Rougeulle, C. and Avner, P. (2008). Molecular coupling of Xist regulation and pluripotency. *Science* **321**, 1693-5.

Navarro, P., Pichard, S., Ciaudo, C., Avner, P. and Rougeulle, C. (2005). Tsix transcription across the Xist gene alters chromatin conformation without affecting Xist transcription: implications for X-chromosome inactivation. *Genes Dev* **19**, 1474-84.

Nesterova, T. B., Johnston, C. M., Appanah, R., Newall, A. E., Godwin, J., Alexiou, M. and Brockdorff, N. (2003). Skewing X chromosome choice by modulating sense transcription across the Xist locus. *Genes Dev* **17**, 2177-90.

Newall, A. E., Duthie, S., Formstone, E., Nesterova, T., Alexiou, M., Johnston, C., Caparros, M. L. and Brockdorff, N. (2001). Primary non-random X inactivation associated with disruption of Xist promoter regulation. *Hum Mol Genet* **10**, 581-9.

Niwa, H., Toyooka, Y., Shimosato, D., Strumpf, D., Takahashi, K., Yagi, R. and Rossant, J. (2005). Interaction between Oct3/4 and Cdx2 determines trophectoderm differentiation. *Cell* **123**, 917-29.

Nothias, J. Y., Majumder, S., Kaneko, K. J. and DePamphilis, M. L. (1995). Regulation of gene expression at the beginning of mammalian development. *J Biol Chem* **270**, 22077-80.

Okamoto, I., Otte, A. P., Allis, C. D., Reinberg, D. and Heard, E. (2004). Epigenetic dynamics of imprinted X inactivation during early mouse development. *Science* **303**, 644-9.

Okamoto, I., Patrat, C., Thepot, D., Peynot, N., Fauque, P., Daniel, N., Diabangouaya, P., Wolf, J. P., Renard, J. P., Duranthon, V. et al. (2011). Eutherian mammals use diverse strategies to initiate X-chromosome inactivation during development. *Nature*.

Okamoto, I., Tan, S. and Takagi, N. (2000). X-chromosome inactivation in XX androgenetic mouse embryos surviving implantation. *Development* **127**, 4137-45.

Oswald, J., Engemann, S., Lane, N., Mayer, W., Olek, A., Fundele, R., Dean, W., Reik, W. and Walter, J. (2000). Active demethylation of the paternal genome in the mouse zygote. *Curr Biol* **10**, 475-8.

Ouyang, Y., Salstrom, J., Diaz-Perez, S., Nahas, S., Matsuno, Y., Dawson, D., Teitell, M. A., Horvath, S., Riggs, A. D., Gatti, R. A. et al. (2005). Inhibition of Atm and/or Atr disrupts gene silencing on the inactive X chromosome. *Biochem Biophys Res Commun* **337**, 875-80.

Patrat, C., Okamoto, I., Diabangouaya, P., Vialon, V., Le Baccon, P., Chow, J. and Heard, E. (2009). Dynamic changes in paternal X-chromosome activity during imprinted X-chromosome inactivation in mice. *Proc Natl Acad Sci U S A* **106**, 5198-203.

Pawson, T. and Scott, J. D. (1997). Signaling through scaffold, anchoring, and adaptor proteins. *Science* **278**, 2075-80.

Penny, G. D., Kay, G. F., Sheardown, S. A., Rastan, S. and Brockdorff, N. (1996). Requirement for Xist in X chromosome inactivation. *Nature* **379**, 131-7.

Plath, K., Talbot, D., Hamer, K. M., Otte, A. P., Yang, T. P., Jaenisch, R. and Panning, B. (2004). Developmentally regulated alterations in Polycomb repressive complex 1 proteins on the inactive X chromosome. *J Cell Biol* **167**, 1025-35.

Plusa, B., Piliszek, A., Frankenberg, S., Artus, J. and Hadjantonakis, A. K. (2008). Distinct sequential cell behaviours direct primitive endoderm formation in the mouse blastocyst. *Development* **135**, 3081-91.

Rappold, G. A. (1993). The pseudoautosomal regions of the human sex chromosomes. *Hum Genet* **92**, 315-24.

Rastan, S. and Robertson, E. J. (1985). X-chromosome deletions in embryo-derived (EK) cell lines associated with lack of X-chromosome inactivation. *J Embryol Exp Morphol* **90**, 379-88.

Rea, S., Xouri, G. and Akhtar, A. (2007). Males absent on the first (MOF): from flies to humans. *Oncogene* **26**, 5385-94.

Reinius, B., Shi, C., Hengshuo, L., Sandhu, K. S., Radomska, K. J., Rosen, G. D., Lu, L., Kullander, K., Williams, R. W. and Jazin, E. (2010). Female-biased expression of long non-coding RNAs in domains that escape X-inactivation in mouse. *BMC Genomics* **11**, 614.

Rice, W. R. (1994). Degeneration of a nonrecombining chromosome. *Science* **263**, 230-2.

Royce-Tolland, M. E., Andersen, A. A., Koyfman, H. R., Talbot, D. J., Wutz, A., Tonks, I. D., Kay, G. F. and Panning, B. (2010). The A-repeat links ASF/SF2-dependent Xist RNA processing with random choice during X inactivation. *Nat Struct Mol Biol* **17**, 948-54.

Sado, T., Fenner, M. H., Tan, S. S., Tam, P., Shioda, T. and Li, E. (2000). X inactivation in the mouse embryo deficient for Dnmt1: distinct effect of hypomethylation on imprinted and random X inactivation. *Dev Biol* **225**, 294-303.

Sarma, K., Levasseur, P., Aristarkhov, A. and Lee, J. T. (2010). Locked nucleic acids (LNAs) reveal sequence requirements and kinetics of Xist RNA localization to the X chromosome. *Proc Natl Acad Sci U S A* **107**, 22196-201.

Schneider, R. and Grosschedl, R. (2007). Dynamics and interplay of nuclear architecture, genome organization, and gene expression. *Genes Dev* **21**, 3027-43.

Silva, J., Nichols, J., Theunissen, T. W., Guo, G., van Oosten, A. L., Barrandon, O., Wray, J., Yamanaka, S., Chambers, I. and Smith, A. (2009). Nanog is the gateway to the pluripotent ground state. *Cell* **138**, 722-37.

Singer-Sam, J., Chapman, V., LeBon, J. M. and Riggs, A. D. (1992). Parental imprinting studied by allele-specific primer extension after PCR: paternal X chromosome-linked genes are transcribed prior to preferential paternal X chromosome inactivation. *Proc Natl Acad Sci U S A* **89**, 10469-73.

Smith, A. G. (2001). Embryo-derived stem cells: of mice and men. *Annu Rev Cell Dev Biol* **17**, 435-62.

Solter, D. and Knowles, B. B. (1975). Immunosurgery of mouse blastocyst. *Proc Natl Acad Sci U S A* **72**, 5099-102.

Splinter, E., de Wit, E., Nora, E. P., Klous, P., van de Werken, H. J., Zhu, Y., Kaaij, L. J., van Ijcken, W., Gribnau, J., Heard, E. et al. (2011). The inactive X chromosome adopts a unique three-dimensional conformation that is dependent on Xist RNA. *Genes Dev* **25**, 1371-83.

Strumpf, D., Mao, C. A., Yamanaka, Y., Ralston, A., Chawengsaksophak, K., Beck, F. and Rossant, J. (2005). Cdx2 is required for correct cell fate specification and differentiation of trophectoderm in the mouse blastocyst. *Development* **132**, 2093-102.

Sugimoto, M. and Abe, K. (2007). X chromosome reactivation initiates in nascent primordial germ cells in mice. *PLoS Genet* **3**, e116.

Takagi, N. (1978). Preferential inactivation of the paternally derived X chromosome in mice. *Basic Life Sci* **12**, 341-60.

Takagi, N. and Sasaki, M. (1975). Preferential inactivation of the paternally derived X chromosome in the extraembryonic membranes of the mouse. *Nature* **256**, 640-2.

Takagi, N., Yoshida, M. A., Sugawara, O. and Sasaki, M. (1983). Reversal of X-inactivation in female mouse somatic cells hybridized with murine teratocarcinoma stem cells in vitro. *Cell* **34**, 1053-62.

Tam, P. P., Zhou, S. X. and Tan, S. S. (1994). X-chromosome activity of the mouse primordial germ cells revealed by the expression of an X-linked lacZ transgene. *Development* **120**, 2925-32.

Tang, Y. A., Huntley, D., Montana, G., Cerase, A., Nesterova, T. B. and Brockdorff, N. (2010). Efficiency of Xist-mediated silencing on autosomes is linked to chromosomal domain organisation. *Epigenetics Chromatin* **3**, 10.

Tesar, P. J., Chenoweth, J. G., Brook, F. A., Davies, T. J., Evans, E. P., Mack, D. L., Gardner, R. L. and McKay, R. D. (2007). New cell lines from mouse epiblast share defining features with human embryonic stem cells. *Nature* **448**, 196-9.

Thornhill, A. R. and Burgoyne, P. S. (1993). A paternally imprinted X chromosome retards the development of the early mouse embryo. *Development* **118**, 171-4.

Thorogood, N. P. and Brown, C. J. (2010). Active chromatin marks are retained on X chromosomes lacking gene or repeat silencing despite XIST/Xist expression in somatic cell hybrids. *PLoS One* **5**, e10787.

Turner, J. M., Mahadevaiah, S. K., Elliott, D. J., Garchon, H. J., Pehrson, J. R., Jaenisch, R. and Burgoyne, P. S. (2002). Meiotic sex chromosome inactivation in male mice with targeted disruptions of Xist. *J Cell Sci* **115**, 4097-105.

van den Berg, I. M., Laven, J. S., Stevens, M., Jonkers, I., Galjaard, R. J., Gribnau, J. and van Doorninck, J. H. (2009). X chromosome inactivation is initiated in human preimplantation embryos. *Am J Hum Genet* **84**, 771-9.

Vincent-Salomon, A., Ganem-Elbaz, C., Manie, E., Raynal, V., Sastre-Garau, X., Stoppa-Lyonnet, D., Stern, M. H. and Heard, E. (2007). X inactive-specific transcript RNA coating and genetic instability of the X chromosome in BRCA1 breast tumors. *Cancer Res* **67**, 5134-40.

Wang, J., Mager, J., Chen, Y., Schneider, E., Cross, J. C., Nagy, A. and Magnuson, T. (2001). Imprinted X inactivation maintained by a mouse Polycomb group gene. *Nat Genet* **28**, 371-5.

West, J. D., Frels, W. I., Chapman, V. M. and Papaioannou, V. E. (1977). Preferential expression of the maternally derived X chromosome in the mouse yolk sac. *Cell* **12**, 873-82.

Wutz, A. and Jaenisch, R. (2000). A shift from reversible to irreversible X inactivation is triggered during ES cell differentiation. *Mol Cell* **5**, 695-705.

Xue, F., Tian, X. C., Du, F., Kubota, C., Taneja, M., Dinnyes, A., Dai, Y., Levine, H., Pereira, L. V. and Yang, X. (2002). Aberrant patterns of X chromosome inactivation in bovine clones. *Nat Genet* **31**, 216-20.

Yamanaka, Y., Lanner, F. and Rossant, J. (2010). FGF signal-dependent segregation of primitive endoderm and epiblast in the mouse blastocyst. *Development* **137**, 715-24.

Zaratiegui, M., Vaughn, M. W., Irvine, D. V., Goto, D., Watt, S., Bahler, J., Arcangioli, B. and Martienssen, R. A. (2011). CENP-B preserves genome integrity at replication forks paused by retrotransposon LTR. *Nature* **469**, 112-5.

Zhang, Y. and Oliver, B. (2007). Dosage compensation goes global. *Curr Opin Genet Dev* **17**, 113-20.

Zhao, J., Ohsumi, T. K., Kung, J. T., Ogawa, Y., Grau, D. J., Sarma, K., Song, J. J., Kingston, R. E., Borowsky, M. and Lee, J. T. (2010). Genome-wide identification of polycomb-associated RNAs by RIP-seq. *Mol Cell* **40**, 939-53.